



Estimating the Hydrodynamic Characteristics of the Dorado Remote Minehunting Vehicle

George D. Watt

Defence R&D Canada

Technical Memorandum

DRDC Atlantic TM 2002-177

October 2002

Estimating the Hydrodynamic Characteristics of the Dorado Remote Minehunting Vehicle

George D. Watt

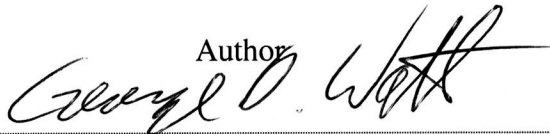
Defence R&D Canada – Atlantic

Technical Memorandum

DRDC Atlantic TM 2002-177

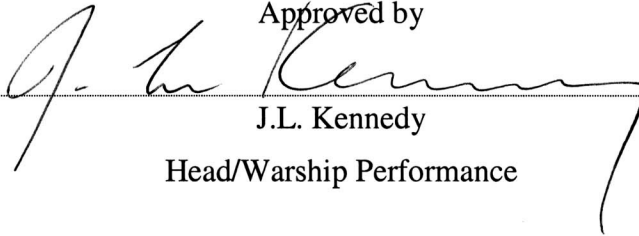
October 2002

Author



George D. Watt

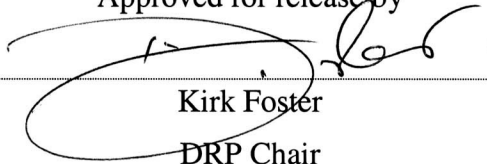
Approved by



J.L. Kennedy

Head/Warship Performance

Approved for release by



Kirk Foster

DRP Chair

The body of this document was prepared using the Maple software package which integrates calculations and text in a single environment. This leads to some deviations from the DRDC standard format.

Abstract

The hydrodynamic forces on the Dorado semi-submersible remote minehunting vehicle are estimated and provided in a form that can be used in a six degree-of-freedom vehicle simulation. The forces apply to either old or new versions of the control planes. The lift (from flow curvature in a turn) and drag of the self-aligning fairings on the snorkel mast are accounted for as a function of vehicle depth. Hydrodynamic coefficients are used for all but the mast effects, where a rational flow model is used. Deficiencies in the control derivatives estimated by the DERIVS/DSSP20 programs are identified and overcome.

Résumé

Les forces hydrodynamiques exercées sur le véhicule semi-submersible Dorado utilisé pour le déminage à distance sont évaluées et fournies sous une forme utilisable dans une simulation de véhicule à six degrés de liberté. Les forces sont appliquées soit à la nouvelle soit à l'ancienne version des plans de commande. La poussée (due à la courbure de l'écoulement dans un virage) et la traînée du carénage à auto-alignement sur le mât du schnorkel sont prises en compte sous la forme d'une fonction de la profondeur du véhicule. Des coefficients hydrodynamiques sont utilisés pour tous les effets, sauf celui du mât, pour lequel un modèle d'écoulement rationnel est utilisé. Des lacunes concernant les paramètres de commande évalués par les programmes DERIVS/DSSP20 sont identifiées et corrigées.

This page intentionally left blank.

Executive summary

Introduction

DRDC Atlantic has developed, and is now supporting a Technology Demonstration Project of a Remote Minehunting System (RMS). The RMS uses a remote drone (called Dorado) to tow a sonar at depths up to 200 m for minehunting and route surveying purposes. DRDC Atlantic has also developed a six degree-of-freedom simulator (SIMRMS) for Dorado, its tow cable, and its towfish. The simulator requires the hydrodynamic characteristics of the RMS components as input. This report estimates these characteristics for the Dorado vehicle.

Principle Results

The Dorado hydrodynamic characteristics are estimated as coefficients and rational flow models. Propulsion effects are not dealt with in this report since further changes to the propulsion system are expected. During the calculations, deficiencies were identified in programs which have been used in the past to estimate control derivatives (depth, pitch, yaw, and roll control authority). Improved algorithms which correct these deficiencies are presented.

Significance of Results

The new Dorado hydrodynamic model should allow SIMRMS to function with improved accuracy. SIMRMS is an important simulation tool in planning and carrying out remote minehunting and route surveying operations.

Future Plans

It is desirable to validate the improved control derivative algorithms through full scale trials with Dorado. Such trials are planned but, as yet, unfunded.

Watt, G.D; 2002; Estimating the Hydrodynamic Characteristics of the Dorado Remote Minehunting Vehicle; DRDC Atlantic TM 2002-177; Defence R&D Canada – Atlantic.

Sommaire

Introduction

R & D pour la défense Canada - Atlantique a mis au point un système de déminage à distance (SDD) dans le cadre d'un projet de démonstration de technologie et il fournit actuellement le soutien à ce système. Le SDD utilise un engin télécommandé (appelé Dorado) pour remorquer un sonar à des profondeurs pouvant atteindre 200 m à des fins de déminage et de levé des routes de navigation. R & D pour la défense Canada - Atlantique a également mis au point un simulateur à six degrés de liberté (SIMRMS) pour le Dorado, son câble de remorquage et son sonar remorqué. Il faut fournir au simulateur les caractéristiques hydrodynamiques des éléments du SDD. Dans le présent rapport, on évalue ces caractéristiques pour le véhicule Dorado.

Principaux résultats

Les caractéristiques hydrodynamiques du Dorado sont évaluées sous forme de coefficients et de modèles d'écoulement rationnel. Le rapport ne traite pas des effets de la propulsion, étant donné que d'autres changements sont prévus au système de propulsion. Lors des calculs, on a identifié des lacunes dans les programmes utilisés par le passé pour évaluer les paramètres de commande (profondeur, tangage, lacet et roulis). Des algorithmes améliorés qui corrigent ces lacunes sont présentés.

Signification des résultats

Le nouveau modèle hydrodynamique du Dorado devrait permettre d'obtenir une plus grande précision avec le SIMRMS. Ce dernier est un important outil de simulation pour la planification et l'exécution des opérations de déminage à distance et de levé des routes de navigation.

Plans pour l'avenir

Il est souhaitable que les algorithmes améliorés relatifs aux paramètres de commande soient validés par des essais en vraie grandeur avec le Dorado. Ces essais sont prévus, mais il n'y a pas encore eu de fonds consacrés à leur exécution.

Watt, G.D; 2002; Estimating the Hydrodynamic Characteristics of the Dorado Remote Minehunting Vehicle; DRDC Atlantic TM 2002-177; Defence R&D Canada – Atlantic.

Table of contents

Abstract	i
Résumé	i
Executive summary.....	iii
Sommaire	iv
Table of contents	v
List of figures	vii
List of symbols.....	ix
Introduction	1
DERIVS/DSSP20 Steady State Predictions.....	3
Correcting the Steady State Derivatives.....	5
Mastless Drag Correction	5
Tailplane Control Derivative Corrections.....	5
Sternplane Pitch Control.....	7
Sternplane Roll Control.....	8
Rudder Control	11
Foreplane Control Derivative Corrections.....	13
Mast Drag.....	16
Dimensionless Mast Drag Forces.....	23
Mast Lift.....	23

Unsteady (Added Mass) Derivatives	28
Concluding Remarks	32
References.....	33
Appendix A: The Dorado DSSP20 and ESAM Input Files	34
DSSP20.....	34
ESAM	36
Appendix B: The Dorado Mastless Steady State Derivatives.....	37
Appendix C: Mast Drag and Lift Code.....	38
Appendix D: Dorado Build 1 Derivatives	39
Sternplane Control Derivative Corrections.....	39
Sternplane Pitch Control.....	39
Sternplane Roll Control.....	40
Foreplane Control Derivative Corrections.....	40
DSSP20 Input File.....	42
Steady State Derivatives.....	43
ESAM Input file.....	44
Unsteady Derivatives.....	44

List of figures

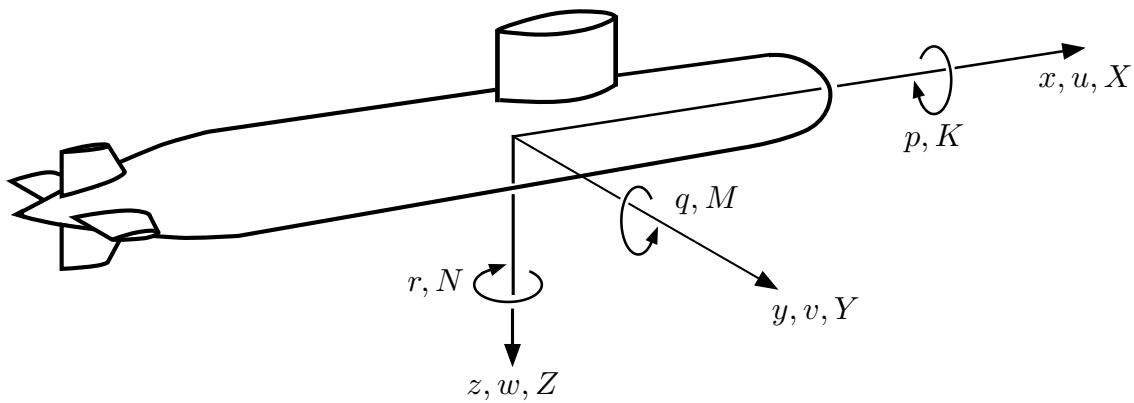
Figure 1. The CRMS Concept (showing the older DOLPHIN Mk2 drone)	2
Figure 2a. Dorado DSSP20 Geometry, Elevation View	3
Figure 2b. Dorado DSSP20 Geometry, View From Below	3
Figure 2c. Dorado DSSP20 Geometry, View From Astern.....	4
Figure 3. Roll Control with an Isolated Wing (W), a Wing and Body (WB), and a Wing, Body, and Fin (WBF)	10
Figure 4. Mast Coordinates and Vehicle Pitch and Roll Euler Angles	16
Figure 5. Streamline Curvature Induced Side Force on the Dorado Self-Aligning Fairing	24
Figure 6. Dorado ESAM Input (black) and Ellipsold (red) Geometry	29

This page intentionally left blank.

List of Symbols

a	isolated wing (exposed wing area) effective aspect ratio $(b - d)^2/S_a$.
A	isolated wing (embedded in hull) effective aspect ratio b^2/S_A .
b	fore or sternplane tip-to-tip span length.
c	wing chord length (mean chord unless subscripted).
C_L, C_D	wing lift and drag coefficients, nondimensionalized with S .
C_f	foreplane depth control derivative correction.
C_{iu}, C_{id}	control derivative corrections, for uniform and differential deflections; $i = s$ for sternplane or r for rudder.
C_{rK}	net rudder roll control derivative correction.
C_ℓ	2D airfoil section lift coefficient, nondimensionalized by chord length.
d	local hull diameter.
d_i	local drag at i ; $i = s$ for surface, b for base, or pm for profile per meter.
D	drag.
D_{Fi}	corrections accounting for discrepancy in Z_w .
F_{ax}, F_{lat}	local axial and lateral force functions.
f_{ax}, f_{lat}	second order approximations to F_{ax}, F_{lat} .
$f_c = c C_\ell / \ell^2$	converts C_ℓ to standard dimensionless form per meter of mast length (with dimensions m^{-1}).
$f_0 = R f_c$	nondimensionalizes f_c .
I_{ax}, I_{lat}	integrals of f_{ax}, f_{lat} over the wetted mast length.
Iz_{ax}, Iz_{lat}	integrals of $z f_{ax}, z f_{lat}$ over the wetted mast length.
K, M, N	body fixed roll, pitch and yawing moments, nondimensionalized with $\rho U^2 l^3 / 2$ (see figure below).
$K_{W(B)}, K_{B(W)}$	ratios of lift on the wing (in the presence of the body) and lift on the body (in the presence of the wing) to the lift on an isolated wing based on <i>exposed</i> wing area S_a .
l	overall hull length.
L	lift.
L_α, L_δ	lift due incidence α or deflection δ ; not derivatives.
p, q, r	body fixed roll, pitch, and yaw angular velocities (see figure below).
r_m	hull radius opposite mast.
R	turning radius of vehicle.
s_m	snorkel mast wetted length.
S	wing planform area.
u, v, w	forward, lateral, and vertical body axes velocities (see figure below).
U	overall velocity: $\sqrt{u^2 + v^2 + w^2}$.

$W(\lambda, A)$	dimensionless rolling moment from an isolated wing with differentially deflecting tips.
$WB(\lambda, A)$	dimensionless rolling moment from differentially deflecting horizontal wings on a body.
$WBF(\lambda, A)$	dimensionless rolling moment from differentially deflecting horizontal wings on a body with fixed vertical fin.
x, y, z	standard body fixed axes.
x_m	body fixed x coordinate of snorkel mast.
z_0	inertial coordinate giving depth of body fixed axes origin.
X, Y, Z	body fixed axial, lateral, and normal forces, nondimensionalized with $\rho U^2 l^2 / 2$ (see figure below).
α	angle of attack: $\tan^{-1}(w/u)$
δ	control surface deflection angle.
η	2D section profile coordinate normal to chord: $\eta(\xi)$.
θ, ϕ	body axes pitch and roll Euler angles.
λ	local hull diameter to span ratio: d/b .
ξ	2D section chordwise coordinate.
ρ	fluid density.
Ω	sweepback angle of wing quarter chord line.



Introduction

The Canadian Remote Minehunting System (CRMS) technology demonstrator consists of a remote drone (called Dorado, 8.2 m long) towing a towfish (3 m long) at depths to 200 m. The towfish carries a sonar which is used for surveying and minehunting purposes. The CRMS promises to be a low cost, low risk way of minehunting (Figure 1).

To help evaluate the system and examine maneuvering strategies, DRDC Atlantic has developed the SIMRMS simulator [1] which provides a six degree-of-freedom dynamic computer simulation of the two vehicles, the tow cable connecting them, and the control systems they use. The equations of motion in this simulation require a description of the hydrodynamic forces on the vehicle. This description is provided primarily in the form of hydrodynamic coefficients (derivatives) but some rational flow modelling can also be used.

This report is concerned with estimating the hydrodynamic forces for the proposed Build 3 version (Fall 2002) of Dorado. The Build 3 version is assumed to include the new, enlarged fore and sternplanes [2], but a version of the forces is also provided for the original Dorado (Build 1) fore and sternplane geometry. The report is not concerned with propulsion forces or the hydrodynamics of the tow cable or the towfish.

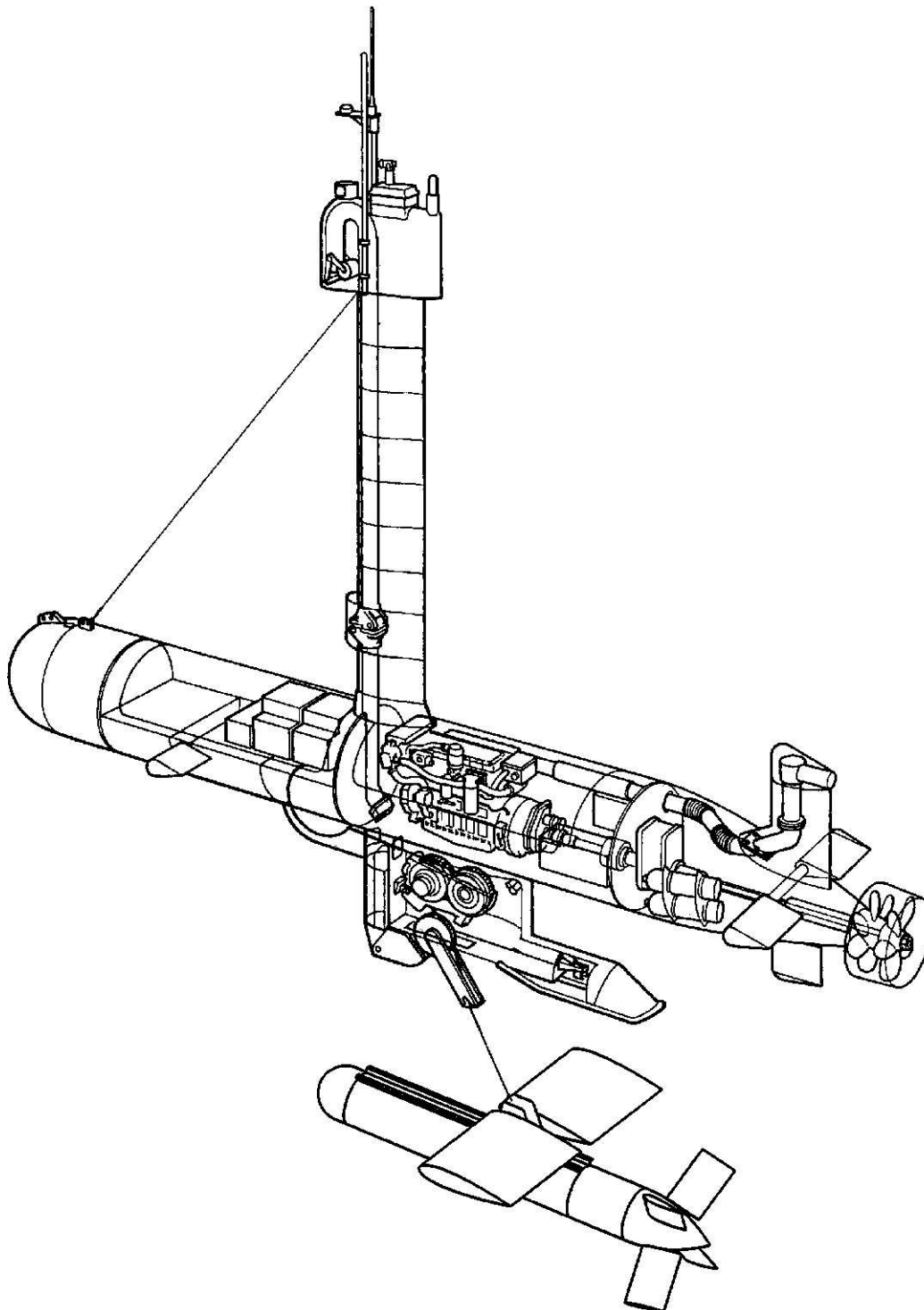
The hydrodynamic forces are initially estimated as derivatives by the DERIVS program [3] which calls the DREA Submarine Simulation Program (DSSP20) [4] to obtain estimates of the steady state hydrodynamic forces. The ESAM program (Estimate Submarine Added Masses) [5] provides estimates of the acceleration coefficients (added mass effects).

While DSSP20 is the basis for the steady state derivatives, its calculations require corrections in two areas. First, it is unable to predict the drag on the unconventional Dorado hull with its many fittings, protrusions, and holes. Secondly, control deflection efficiency in the current version (June 2001) is incorrectly modelled. In addition to these corrections, the Dorado snorkel mast with its self aligning fairings cannot be handled at all by DSSP20. These effects are calculated manually.

The mast effects are particularly challenging for two reasons. First, all the mast forces are a function of vehicle depth (ie, the wetted length of the mast). The snorkel mast extends through the free surface and experiences considerable drag, both along its length and right at the free surface (wave and ventilation drag). So, for example, the pitch-up moment caused by the mast varies with depth, something that has been observed by the operators. Note that the wave drag modelled here is wave drag from the mast, not from the main vehicle. This latter effect is thought to be small (the hull is two to three diameters below the free surface) and it is not modelled at the present time.

The second reason the mast is a challenging appendage to model is that, although its self-aligning fairings do not generate lift in a translating flow, they do generate lift when the vehicle turns. This lift results from the curved streamlines interacting with the symmetrical fairing. The lift is reversed and amplified by the self-aligning mechanism, causing the vehicle to roll to the outside of the turn.

Fig. 1: The CRMS Concept (showing the older DOLPHIN Mk2 drone)



DERIVS/DSSP20 Steady State Predictions

DSSP20 builds a hydrodynamic model of the flow around a streamlined vehicle based on an input file describing nothing but vehicle geometry. The input file for Dorado is shown in Appendix A and its format is described by Mackay [4]. This geometry is shown below in Figure 2:

Fig. 2a: Dorado DSSP20 Geometry (No Mast), Elevation View

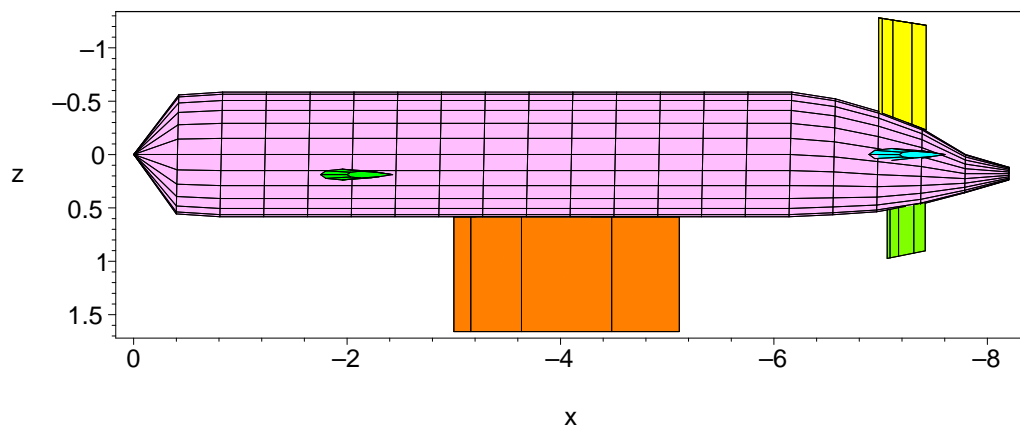


Fig. 2b: Dorado DSSP20 Geometry (No Mast), View From Below

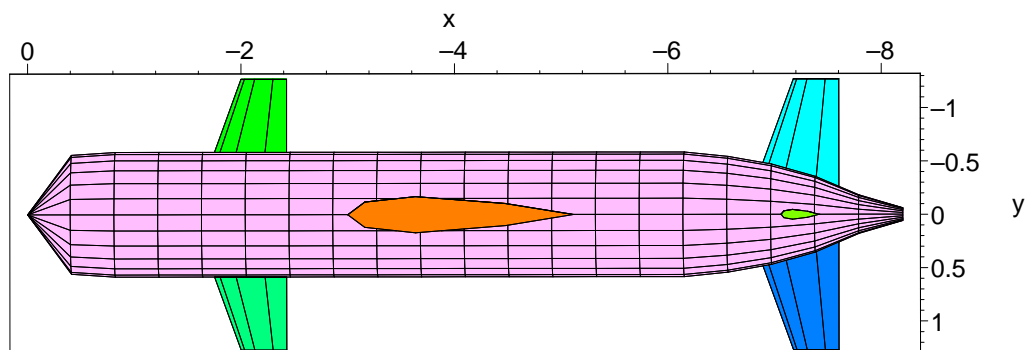
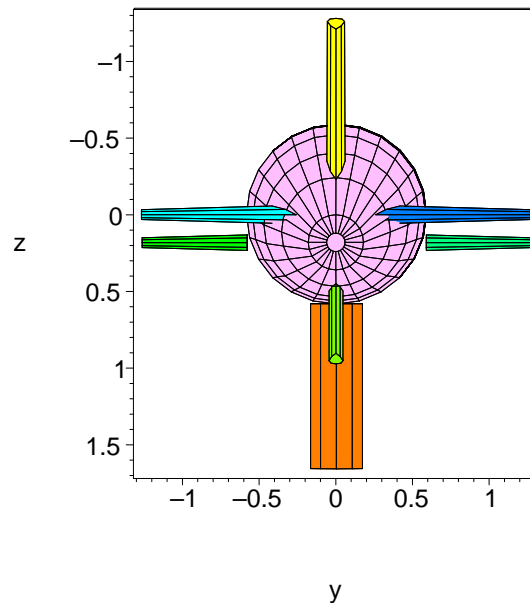


Fig. 2c: Dorado DSSP20 Geometry (No Mast), View From Astern



DSSP20 deals with the vehicle component by component (hull, starboard sternplane, port sternplane, etc.) and each component is shown as a different color in these figures. Only the overall component geometry is important so, for example, modelling the hemi-spherical cap at the nose of the hull is unnecessary. Note the absence of the mast.

The foreplanes in Figure 2 deflect together to provide depth control. The vertical stabilizer above the hull at the aft end is fixed and houses the diesel engine exhaust. The rudder is the single appendage below the tail. The sternplanes provide both pitch and roll control. The fore and sternplanes shown here double the depth, pitch, and roll control authority relative to the Build 1 design [2].

The DERIVS `derivs.dat` input file, described in detail by Watt [3], is short:

```
dorado
no, do not zero residual drag
8.2 1025. 5.144
defv ds: 1 1.0 2 -1.0
defh do: 1 -1.0 2 -1.0
defv df: 3 1.0 4 -1.0
defh dr: 5 1.0
```

It gives the root file name for DSSP20 input and output files, direction on how to handle a truncated stern, the vehicle length, fluid density, and speed (all in SI units), and then four lines defining vertical and horizontal plane control deflections. The `ds`, `do`, `df`, and `dr` deflections define how pitch control (uniform sternplane deflection `ds`), roll control (differential sternplane deflection `do`), depth control (uniform foreplane deflection `df`), and yaw control (rudder deflection `dr`) are implemented by appendages 1 through 5 in the DSSP20 input file.

DERIVS outputs a set of hydrodynamic coefficients (first and second order derivatives) in the body fixed axes shown in Figure 2, except the origin is shifted aft, on the hull

centerline, approximately opposite the hull center of buoyancy. Feldman [6] shows how these derivatives are nondimensionalized and used in the equations of motion.

In the next section, the DERIVS output is corrected and enhanced to better model drag, control, and the lift and drag effects of the mast. The fully corrected steady state hydrodynamic derivatives are presented in Appendix B.

Correcting the Steady State Derivatives

The DERIVS generated derivatives are adjusted to:

- correct vehicle drag,
- correct appendage control derivatives,
- correct foreplane effectiveness,
- include effect of mast drag as a function of depth and vehicle orientation,
- include side force generated on the mast self-aligning fairings in curved flow (ie, when the vehicle turns) also as a function of depth.

Mastless Drag Correction

Mastless drag is based on full scale trials with the DOLPHIN Mk 1 vehicle [7]. In these trials, the DOLPHIN vehicle was driven with an electric motor with and without the mast on. With the vehicle travelling at 10 knots, the mastless drag (hull plus all appendages except the snorkel mast) was 542 lb. This gives a dimensionless mastless axial force coefficient:

$$X_{\text{experiment, Mk 1, no mast}}^* = 2 \frac{\text{drag}}{\rho l^2 U^2} = -.003288$$

The DERIVS estimate for the Mk1 X^* coefficient is:

$$X_{\text{DERIVS, Mk 1, no mast}}^* = -.00173$$

The difference, ΔX^* , is due to the abnormal shape of the Mk1 hull, its many attachments, external latch handles, holes and slots in the hull, external weldments, etc:

$$\Delta X^* = -.001558$$

This difference is simply added to the Dorado X^* coefficient predicted by DERIVS.

Tailplane Control Derivative Corrections

DSSP20 (June 2001 version) predicts tailplane effectiveness (the contribution of the tailplanes to the transverse force when the vehicle is at incidence) correctly but

overpredicts tailplane control derivatives. It assigns an all-moving sternplane the same lift increment for a control δ_s deflection as for a vehicle angle of attack α deflection. In the former case, only the sternplanes deflect relative to the flow while in the latter both hull and sternplanes deflect. The former case generates substantially less lift than the latter case. And there is a further substantial lift reduction required to correctly model differential deflections (for roll control). For pitch control, equal lift on simultaneously deflected sternplanes reinforces itself across the body, but the opposing lift from differential deflections negates itself at the center.

Pitts *et al* [8] use slender body theory to show that the lift generated on a slender cylindrical body and wing combination due to incidence α is:

$$L_\alpha = (K_{W(B)} + K_{B(W)}) L_W$$

where:

$$K_{W(B)} + K_{B(W)} = (1 + \lambda)^2$$

$$\lambda = \frac{d}{b}$$

and L_W is the lift on the exposed wing area with body removed and exposed wings joined at the centerline, $K_{W(B)}$ is a dimensionless coefficient giving the lift on the wing in the presence of the body, and $K_{B(W)}$ gives the carry-over lift on the body in the presence of the wing. The λ parameter is the ratio of the hull diameter d to wing tip-to-tip span b (for the body and wing combination) so that $0 < \lambda < 1$.

Pitts *et al* also quote the results for lift due to deflection δ and these can be simplified to:

$$L_\delta = K_{W(B)} L_W$$

so that:

$$\frac{L_\delta}{L_\alpha} = \frac{1}{1 + \frac{K_{B(W)}}{K_{W(B)}}}$$

Analytical expressions derived from slender body theory are available for $K_{W(B)}$ and $K_{B(W)}$ and are presented by Pitts *et al*. However, it is approximately true that:

$$\frac{K_{B(W)}}{K_{W(B)}} = \lambda + \frac{1}{5} \lambda (1 - \lambda) + \text{higher order terms}$$

To first order, this ratio is just λ which exactly matches the slender body theory

expression at $\lambda=0$ and 1 . The quadratic term in λ on the RHS is a second order (small perturbation) correction. Coupling this expression with that for the $K_{W(B)} + K_{B(W)}$ given above, it is asymptotically consistent that:

$$K_{W(B)} = 1 + \lambda - \frac{1}{5} \lambda (1 - \lambda)$$

Similarly:

$$\frac{L_{\delta}}{L_{\alpha}} = \frac{1}{1 + \lambda} - \frac{1}{5} \frac{\lambda (1 - \lambda)}{(1 + \lambda)^2}$$

As the appendage span b goes to infinity ($\lambda \rightarrow 0$), there is no difference between δ and α deflections; the hull is inconsequential. But as the span becomes increasingly small ($b \rightarrow d$, $\lambda \rightarrow 1$), a δ deflection generates only half the lift that is generated when the hull deflects as well.

Sternplane Pitch Control

Let C_{su} be the correction that needs to be applied to the DERIVS sternplane pitch control (δ_s) derivatives (s for sternplane, u for uniform deflection). Since these derivatives erroneously use $L_{\delta} = L_{\alpha}$, they are corrected by multiplying by:

$$C_{su} = \left(\frac{L_{\delta}}{L_{\alpha}} \right)_{correct}$$

$$= \frac{1}{1 + \lambda} - \frac{1}{5} \frac{\lambda (1 - \lambda)}{(1 + \lambda)^2}$$

That is:

$$L_{\delta_{correct}} = C_{su} L_{\delta_{DERIVS}}$$

We get:

$$b = 2.53708, \quad d = .96844, \quad \lambda = .3817$$

$$C_{su} = .6990$$

where λ is calculated using the hull diameter d at the root leading edge. Recent experiments suggest this as a way to empirically correct for the boundary layer.

This correction is applied as is to Z_{δ_s} and M_{δ_s} . The remaining δ_s control derivatives are second order X and M derivatives. They result primarily from induced drag which increases as the square of the lift on the appendage. Therefore, the X and $M \delta_s$ derivatives are corrected by multiplying by C_{su}^2 .

Sternplane Roll Control

There are two further effects that need to be accounted for with differential deflections. First, the rolling moment from each half of a simple low aspect ratio wing deflecting uniformly across its centerline (so that the moments oppose each other and the net moment is zero) is twice that when each half deflects differentially (when the moments have the same sign; see De Young [9]). This is because the lift (pressure distribution) for uniform deflection reinforces itself across the centerline and is actually greatest there, whereas the lift for differential deflections cancels at the centerline.

Second, with uniform sternplane deflections, the velocity field that is generated is symmetrical about the vertical centerplane through the hull. So there is no interference with the vertical tailplane appendages. For differential sternplane deflections, however, crossflow is present at the centerplane (resulting from sternplane tip and strong hull bound vorticity) which generates a moment on the vertical appendages counteracting the moment developed by the sternplanes themselves (Adams and Dugan [10]).

So there are three good reasons why roll control is best implemented with ailerons located well outboard of the hull centerline:

- differential lift (opposing pressure distributions) is not compromised by close proximity of the lifting components,
- crossflow on the centerplane is minimized, thereby minimizing roll reduction from interaction of the crossflow with vertically oriented appendages on the centerplane, and
- rolling moment is maximized because of the larger moment arm.

For these reasons, it makes good sense to implement roll control on the Dorado mast rather than its sternplanes. Doing so provides the added benefit of allowing the sternplanes to be devoted entirely to pitch control. However, roll control on the mast requires an additional system and this prevents its consideration at this time.

De Young [9] uses slender body theory to analyse the roll control generated by differentially deflected components on an isolated wing. If the deflecting components are symmetrical about the centerline and are the all-movable ends of the wing, and λ is the ratio of the nondeflecting inner portion of the span length to the overall span length, then the dimensionless rolling moment generated by differentially deflecting each wing component an angle δ_o is:

$$W(\lambda, A) = 2 \frac{\frac{\partial}{\partial \delta_o} \text{moment}}{\rho U^2 S b}$$

$$= \frac{1}{6} (1 - \lambda^2)^{(3/2)} A$$

where $W(\lambda, A)$ is a ‘wing’ alone function, $S = bc$ is the wing surface area, $A = b^2/S = b/c$ is the aspect ratio of the wing, and c is the mean chord length.

When the nondeflecting inner portion is replaced with a circular body, so the deflecting ends of the wing are now sternplanes, Adams and Dugan [10] use slender body theory to show that the dimensionless moment $WB(\lambda, A)$ (for ‘wing and body’) is a complicated numerical integration of an elliptic function. Their plotted results can be fit with:

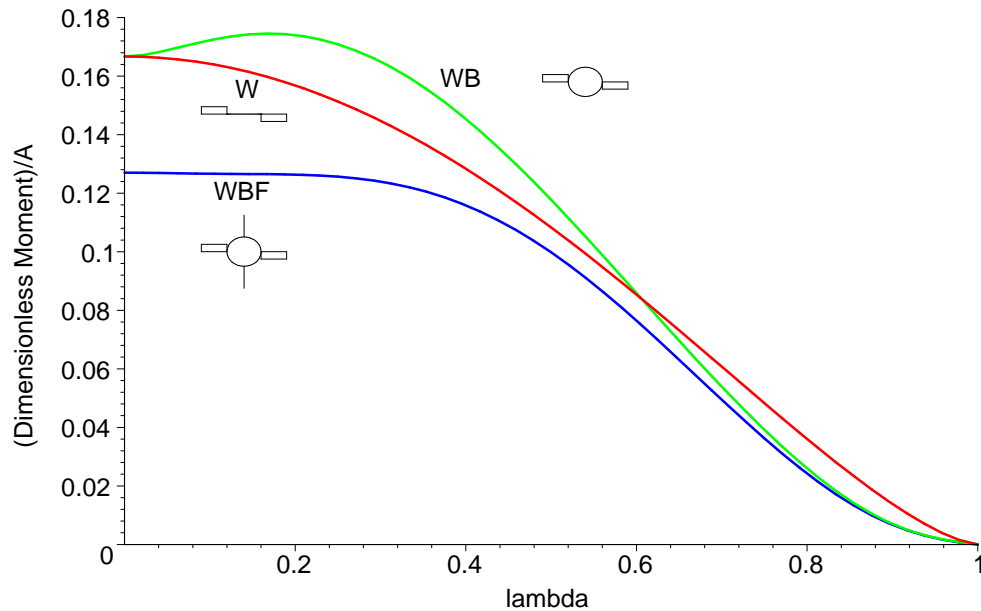
$$WB(\lambda, A) = \left(\frac{1}{6} (1 - \lambda^2)^{(3/2)} + .720 \lambda^2 (1 - \lambda)^{10} + .819 \lambda^2 (1 - \lambda)^3 \right. \\ \left. - .520 \lambda^3 (1 - \lambda)^2 - 1.306 \lambda^{12} (1 - \lambda)^2 \right) A$$

Adams and Dugan also include the effect of the vertical fin (having the same planform as the sternplanes) on the moment generated by differentially deflecting sternplanes:

$$WBF(\lambda, A) = (.127 (1 - \lambda^2)^{(3/2)} + 2.043 \lambda^2 (1 - \lambda)^2 - 1.979 \lambda^2 (1 - \lambda)^4 \\ - 2.543 \lambda^3 (1 - \lambda)^2 - .661 \lambda^{13} (1 - \lambda)^2) A$$

These three functions are shown in the next figure.

**Fig. 3: Roll Control with an Isolated Wing (W),
a Wing and Body (WB), and a Wing, Body, and Fin (WBF)**



Adding a body to the wing apparently has two major effects. First, it helps to isolate, and therefore maintain, the opposing loads. This effect tends to increase the moment and it dominates for small body diameters when the opposing loads are close to each other. Second, it reduces the amount of lift supported by the adjacent portion of the inner, nondeflecting part of the wing. This effect is only seen for large nondeflecting inner span lengths, when λ approaches 1 and the opposing loads are at the ends of the wings well away from one another.

Adding a vertical fin reduces the moment since the fin resists the circulation field the deflecting sternplanes generate.

Adams and Dugan note that if the vertical fin also sustains a differential deflection δ_o , then the net moment generated is $2 \text{ WBF}(\lambda, A)$. In linearized slender body theory, the principle of superposition applies.

Dorado's vertical appendages are smaller than its sternplanes, so the vertical appendages counteract the sternplane induced roll less than if, as the WBF function assumes, they had the same planforms as the sternplanes. However, this decrease in the reduction is assumed to be negligible since the missing span length is well away from the body and, therefore, also the sternplane induced circulation impinging on the vertical fins.

DSSP20 assumes that roll control is simply the lift that would be generated on a single appendage with the vehicle at incidence times $4/(3\pi)$ of the half span length (the

spanwise center of pressure for half the lift, assuming an elliptic lift distribution) times 2, since there are two sternplanes. This calculation accounts for the effect of the boundary layer and afterbody contraction on tailplane efficiency. The correction that needs to be applied to the DSSP20 prediction, therefore, is the ratio of the slender body theory prediction of actual roll control moment ($WBF(\lambda, A)$) to that from incidence lift acting at the $4/(3\pi)$ spanwise location. This latter moment is $K_{W(B)} + K_{B(W)} = (1 + \lambda)^2$ times the slender body theory prediction of dimensionless lift on half the exposed wing ($\pi a/4$ where a is the aspect ratio of the exposed sternplanes joined together), times S_a / S_A to convert the nondimensionalization of this latter lift from an area based on the exposed sternplanes to one based on the full span planes, times the dimensionless moment arm $4/(3\pi)/2$, times 2 because there are two sternplanes:

$$2 \times \text{moment from incidence lift on one sternplane} = \frac{1}{3} \frac{(1 + \lambda)^2 a S_a}{S_A}$$

$$= \frac{1}{3} A (1 - \lambda^2)^2$$

since:

$$\frac{a S_a}{A S_A} = \frac{(b - d)^2}{b^2}$$

So, the correction C_{sd} (d for differential) to be applied to DERIVS δ_o derivatives depends only on λ :

$$C_{sd} = 3 \frac{WBF(\lambda, A)}{A (1 - \lambda^2)^2}$$

$$= .4845$$

C_{sd} is applied as is to derivatives linear in δ_o and C_{sd}^2 multiplies those second order in δ_o^2 .

Rudder Control

The single rudder appendage deflects opposite the stationary vertical stabilizer and in the presence of the sternplanes. From a slender body theory perspective, this is a superposition of two effects: the rudder and vertical stabilizer deflecting uniformly $\delta_r/2$ degrees and the two planes deflecting differentially $\delta_r/2$ degrees.

The uniform $\delta_r/2$ deflection determines the side force and yawing moment response. This will be half the response of uniformly deflecting symmetrical rudder appendages

deflecting δ_r degrees. DSSP20 tries to do this but errs in predicting the uniform load in the same way as for uniform sternplane deflection. The correction is, as before, to multiply the DERIVS Y_{δ_r} and N_{δ_r} derivatives by a correction C_{ru} where:

$$C_{ru} = \left(\frac{L_{\delta}}{L_{\alpha}} \right)_{correct}$$

$$= \frac{1}{1+\lambda} - \frac{1}{5} \frac{\lambda(1-\lambda)}{(1+\lambda)^2}$$

$$= .6281$$

where:

$$b = 1.646, \quad d = .89, \quad \lambda = .5407$$

with d again the local hull diameter opposite the leading edge root location.

The differential $\delta_r/2$ deflection primarily determines the rolling moment derivative K_{δ_r} . The derivative is half the prediction for symmetrical rudder appendages differentially deflecting δ_r degrees. Again, DSSP20 tries to do this but errs as above for the differential sternplane deflections. The correction is to multiply the derivative by C_{rd} where:

$$C_{rd} = 3 \frac{WBF(\lambda, A)}{A(1-\lambda^2)^2}$$

$$= .5452$$

Actually, the K_{δ_r} derivative also has a contribution from the Y_{δ_r} derivative since the Dorado stern droops. That is, the center of the imaginary symmetrical pair of rudders uniformly deflecting $\delta_r/2$ degrees is 0.077 m below the centerline of the hull (at the rudder leading edge) about which the rolling moment is calculated. So the DERIVS K_{δ_r} derivative is actually calculated from:

$$L_{\alpha} \left(\frac{2}{3} \frac{b}{\pi} + .077 \right)$$

so that $0.077/(0.077+2b/3\pi)$ of the DERIVS K_{δ_r} derivative is attributable to uniform

loading and therefore requires the C_{ru} correction, and the remainder is attributable to differential loading and requires the C_{rd} correction. Therefore, the net correction to K_{δ_r} is:

$$\begin{aligned} C_{rK} &= .1806 C_{ru} + .8194 C_{rd} \\ &= .5602 \end{aligned}$$

which is not very different from the previous calculation.

The DERIVS Y_{δ_r} and N_{δ_r} derivatives are corrected by multiplying by C_{ru} . The K_{δ_r} derivative is corrected by multiplying by C_{rK} . The X and M second order δ_r derivatives are inherently nonlinear and no linear theory or superposition argument can explain how to correct them. A second order correction that is some kind of average of the C_{ru} and C_{rK} correction terms seems appropriate, however, and so we use the simple product $C_{ru} C_{rK}$ to correct the second order derivatives.

Foreplane Control Derivative Corrections

The DERIVS estimated foreplane control derivatives are known to be underestimated. In this section, we recalculate foreplane effectiveness to see where the error occurs. The methods of Pitts *et al* [8] again form the basis of the analysis.

The lift generated by the foreplanes due to an angle of attack α is modelled via:

$$\begin{aligned} L_\alpha &= (K_{W(B)} + K_{B(W)}) L_W \\ &= (1 + \lambda)^2 L_W \end{aligned}$$

as described in the previous section. The lift L_W is the lift on the exposed appendages with the body removed and the appendages joined at the centerline (the ‘wing alone’). This lift is estimated using Whicker and Fehlner’s [11] expression for the lift on a low aspect ratio isolated wing:

$$\frac{\partial}{\partial \alpha} C_L = 1.8 \frac{\pi a}{1.8 + \cos(\Omega) \sqrt{\frac{a^2}{\cos(\Omega)^4} + 4}}$$

where:

$$C_L = 2 \frac{L}{\rho U^2 S_a}$$

and Ω is the sweepback of the quarter-chord line. This gives the foreplane

contribution to the normal force derivative Z_w as:

$$\Delta Z_w = -2 \frac{\frac{\partial}{\partial \alpha} L_\alpha}{\rho U^2 l^2}$$

$$= -1.8 \frac{(1 + \lambda)^2 \pi a S_a}{\left(1.8 + \cos(\Omega) \sqrt{\frac{a^2}{\cos(\Omega)^4} + 4} \right) l^2}$$

But:

$$a S_a = b^2 (1 - \lambda)^2$$

so:

$$\Delta Z_w = -1.8 \frac{(1 - \lambda^2)^2 \pi b^2}{\left(1.8 + \cos(\Omega) \sqrt{\frac{a^2}{\cos(\Omega)^4} + 4} \right) l^2}$$

Since:

$$b = 2.5370 \text{ m}$$

$$a = 2.484$$

$$\lambda = .4605$$

$$\Omega = 15.27 \text{ degrees}$$

the foreplane contribution to Z_w is:

$$\Delta Z_w = -.06697$$

The DERIVS/DSSP20 prediction is 17% larger than this, which seems large but is probably within the error of these estimates.

From the previous section we know that:

$$\frac{L_\delta}{L_\alpha} = \frac{1}{1 + \lambda} - \frac{1}{5} \frac{\lambda (1 - \lambda)}{(1 + \lambda)^2}$$

$$= .6614$$

so that:

$$Z_{\delta_f} = \left(\frac{1}{1+\lambda} - \frac{1}{5} \frac{\lambda(1-\lambda)}{(1+\lambda)^2} \right) \Delta Z_w$$

$$= -.04430$$

And this is 20% larger than the DERIVS/DSSP20 prediction of Z_{δ_f} . That is, the effective DSSP20 prediction for L_{δ}/L_{α} is 0.47 which is too low since we know this ratio achieves a lower limit of 0.5 as $\lambda \rightarrow 1$. A much larger underprediction of Z_{δ_f} occurs with the original Dorado foreplanes, as shown in Appendix D.

Two sets of corrections are made. First, Z_w , M_w , Z_q , and M_q are adjusted by adding the following D_{Z_w} , D_{M_w} , D_{Z_q} , and D_{M_q} values to account for the discrepancy in Z_w :

$$D_{Z_w} = -.06697 - (\Delta Z_w)_{DSSP20}$$

$$= .01120$$

$$D_{M_w} = -\frac{D_{Z_w}(x_{qc} - x_{CB})}{l}$$

$$= -.002322$$

$$D_{Z_q} = D_{M_w}$$

$$= -.002322$$

$$D_{M_q} = -\frac{D_{Z_q}(x_{qc} - x_{CB})}{l}$$

$$= .0004815$$

where $x_{qc} - x_{CB}$ is the distance from the center of buoyancy to the nominal quarter chord location of the foreplanes.

No change is made to drag or second order derivatives as a result of these corrections. The corrections are small and may be explainable by the use of different algorithms. Nevertheless, they are made in order that the derivatives are consistent with the algorithms used to design the foreplanes [2].

The second correction is to Z_{δ_f} which is achieved using the factor:

$$C_f = -0.04430 \frac{1}{Z_{\delta_f}^{DSSP20}}$$

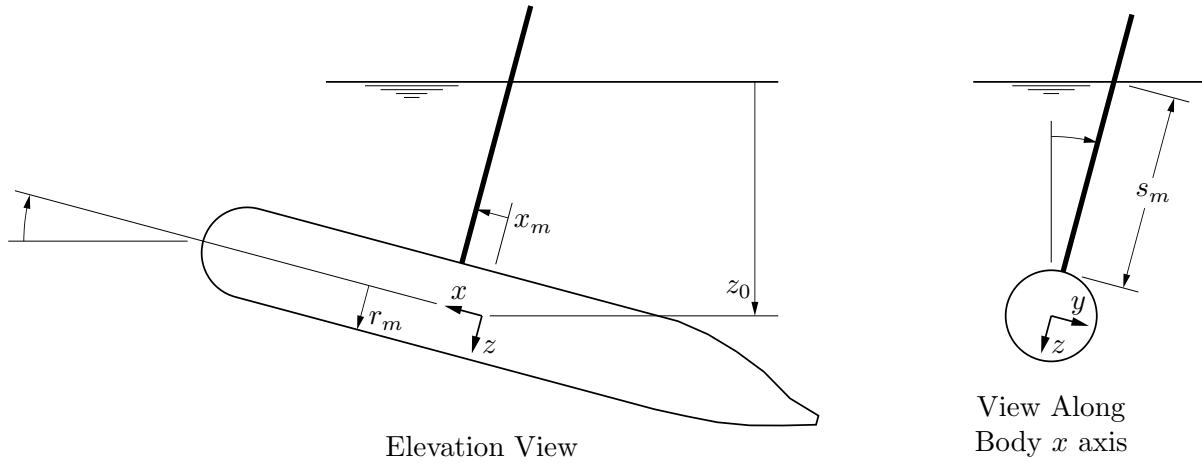
$$= 1.203$$

The linear δ_f derivatives are corrected by multiplying by C_f . The second order δ_f derivatives are corrected by multiplying by C_f^2 .

Mast Drag

The mast forces are a function of the length of the submerged mast, s_m . This varies with the depth of the vehicle and its pitch and roll angles:

Fig. 4: Mast Coordinates and Vehicle Pitch and Roll Euler Angles



$$s_m = \frac{z_0 - x_m \sin(\theta)}{\cos(\theta) \cos(\phi)} - r_m$$

where z_0 is an inertial coordinate giving the depth of the origin of the vehicle body fixed axes, x_m is the axial coordinate of the mast in body fixed axes, θ and ϕ are the vehicle pitch and roll Euler angles, and r_m is the hull radius at the mast:

body axes origin = 3.7 m aft of nose

$$x_m = .4234 \text{ m}$$

$$r_m = .5842 \text{ m}$$

Mast drag is based on full scale trials with the DOLPHIN Mk I vehicle [7]. The DOLPHIN and Dorado self-aligning fairings are geometrically similar, although submerged mast length and other vehicle properties are not. The Dorado mast chord is largest:

$$\frac{\text{Dorado mast chord length}}{\text{DOLPHIN Mk I mast chord length}} = 1.209$$

and the square of this ratio is used to scale experimentally measured DOLPHIN forces to Dorado forces (except for the section profile drag which scales in proportion to the ratio).

In the trials, DOLPHIN was powered by an electric motor with and without the mast attached, allowing the mast drag to be isolated. With the vehicle travelling at 10 knots, the mast drag was 353 lb. The component contributions to this drag are estimated as [7]:

- Ventilation drag (a vent a foot or so deep opens up at the surface behind the fairings) = 120 lb.
- Spray drag = 13 lb.
- Wave drag = 130 lb.

These three drag components act at the surface at (x_m, z_s) in body axis coordinates. They are totaled, scaled to Dorado, and nondimensionalized (using the square of Dorado's hull length) in d_s , the surface component of mast drag:

$$d_s = .001871$$

$$z_s = -r_m - s_m$$

- Junction drag = 13 lb.

This is scaled and nondimensionalized in d_b , which acts at the base of the mast at (x_m, z_b) :

$$d_b = .00009250$$

$$z_b = -r_m$$

- Profile drag = 77 lb.

This is converted to a dimensionless section profile drag d_{pm} (drag per meter) using the fact that the nominal DOLPHIN submerged mast length is 9.5 feet.

$$d_{pm} = .0001565$$

The Dorado profile drag is reconstituted by integrating d_{pm} along the mast in the presence of a local velocity field.

Because the fairings self align, the drag acts locally in the direction of the local flow (assuming there are many separate fairings in the spanwise direction, which is not strictly correct). Mast drag is generated by 5 of the 6 possible vehicle velocities: u, v, p, q, r (see Watt [5]). The first two are the axial and lateral translational velocities; the third translational velocity w (co-axial with the mast), is assumed to not influence drag. The roll, pitch, and yaw rotational velocities p, q, r do contribute to the drag. The influence of all 5 motions on the drag is a function of their integrated effect along the mast in a local flow influenced by the hull.

The axial velocity of the mast u_m is a function of the vehicle axial velocity u , its pitching moment q , and the position along the mast z :

$$u_m = u + q z$$

There is no interference with axial force, assuming the hull is an infinitely long cylinder.

The lateral velocity of the mast v_m depends on the vehicle lateral velocity v , its yaw angular velocity r , its roll angular velocity p , the axial location of the mast x_m , the local hull radius at the mast r_m , and the location along the mast z :

$$v_m = (v + r x_m) \left(1 + \frac{r_m^2}{z^2} \right) - p z$$

The lateral velocity of the hull opposite the mast, $v + r x_m$, generates an interference velocity along the mast which is modelled using the velocity field from 2D potential flow over a circular cylinder. The lateral velocity generated by roll, $-p z$, generates no interference velocity about the axisymmetric hull.

Since crossflow velocity was not present in the trials from which the mast drag components were extracted, the mast drag coefficients are correct as shown above.

With Dorado moving with 6 degrees-of-freedom, the local dimensionless drag force on

the mast is $d_i(u_m^2 + v_m^2)U^2$ where $U^2 = u^2 + v^2 + w^2$. The axial and lateral components of this force are obtained by multiplying by the cosine $u_m / \sqrt{u_m^2 + v_m^2}$ and sine $v_m / \sqrt{u_m^2 + v_m^2}$ of the crossflow angle:

$$\begin{aligned} \text{local axial drag force component} &= \frac{d_i u_m \sqrt{u_m^2 + v_m^2}}{U^2} \\ \text{local lateral drag force component} &= \frac{d_i v_m \sqrt{u_m^2 + v_m^2}}{U^2} \end{aligned}$$

Of course, these forces act in a direction opposite to the u_m and v_m mast velocities.

It is convenient to define axial $F_{ax}(z)$ and lateral $F_{lat}(z)$ functions from these force components for calculating the forces:

$$\begin{aligned} F_{ax}(z) &= u_m \sqrt{u_m^2 + v_m^2} \\ &= (u + qz) \sqrt{(u + qz)^2 + \left((v + rx_m) \left(1 + \frac{r_m^2}{z^2} \right) - pz \right)^2} \\ F_{lat}(z) &= v_m \sqrt{u_m^2 + v_m^2} \\ &= \left((v + rx_m) \left(1 + \frac{r_m^2}{z^2} \right) - pz \right) \sqrt{(u + qz)^2 + \left((v + rx_m) \left(1 + \frac{r_m^2}{z^2} \right) - pz \right)^2} \end{aligned}$$

So, when calculating the forces at the surface, for example, the axial and lateral force components are proportional to $d_s F_{ax}(z_s)$ and $d_s F_{lat}(z_s)$. For the base, the b subscript is used. However, to get the profile drag, $d_{pm} F_i(z)$ needs to be integrated along the length of the mast. And to get the moment generated by the profile drag, we need to multiply the integrand by z . This gives rise to the four integrals calculated below.

Unfortunately, integrals of F_{ax} and F_{lat} cannot be solved analytically. And it is unwieldy to have to do a numerical integration every time step of a simulation. So a conventional expansion of these functions is made before they are integrated. The expanded and truncated functions are designated $f_{ax}(z)$ and $f_{lat}(z)$. The expansion assumes the axial velocity u is much larger than any other velocity component, and third and higher order terms are truncated. Thus, the mast profile drag contribution to the forces is second order accurate, which is consistent with the other derivatives calculated by DERIVS.

The expansion for the axial force function $F_{ax}(z)$ and its associated integrals are:

$$u_m \sqrt{u_m^2 + v_m^2} = u^2 + 2 q z u + \frac{1}{2} v_m^2 + q^2 z^2 + O\left(\frac{v_m^4}{u^2}\right)$$

$$f_{ax}(z) = u^2 + 2 q z u + \frac{1}{2} \left((v + r x_m) \left(1 + \frac{r_m^2}{z^2} \right) - p z \right)^2 + q^2 z^2$$

$$I_{ax} = \int_{z_s}^{z_b} f_{ax}(z) dz$$

$$\begin{aligned} &= u^2 s_m - q u s_m (s_m + 2 r_m) + \frac{1}{3} q^2 s_m (s_m^2 + 3 r_m s_m + 3 r_m^2) \\ &\quad + \frac{\frac{1}{6} s_m (3 s_m^3 + 12 r_m^3 + 24 r_m^2 s_m + 16 r_m s_m^2) (v + r x_m)^2}{(r_m + s_m)^3} \\ &\quad + \frac{1}{2} p (v + r x_m) \left(s_m^2 + 2 r_m s_m + 2 r_m^2 \ln \left(\frac{r_m + s_m}{r_m} \right) \right) + \frac{1}{6} p^2 s_m (s_m^2 + 3 r_m s_m + 3 r_m^2) \end{aligned}$$

$$I_{zax} = \int_{z_s}^{z_b} z f_{ax}(z) dz$$

$$\begin{aligned} &= -\frac{1}{2} u^2 s_m (s_m + 2 r_m) + \frac{2}{3} q u s_m (s_m^2 + 3 r_m s_m + 3 r_m^2) \\ &\quad - \frac{1}{4} q^2 s_m (s_m + 2 r_m) (2 r_m^2 + 2 r_m s_m + s_m^2) - r_m^2 (v + r x_m)^2 \ln \left(\frac{r_m + s_m}{r_m} \right) \end{aligned}$$

$$-\frac{1}{4} \frac{s_m (v + r x_m)^2 (s_m + 2 r_m) (2 r_m^2 + 2 r_m s_m + s_m^2)}{(r_m + s_m)^2}$$

$$-\frac{1}{3} p s_m (s_m^2 + 3 r_m s_m + 6 r_m^2) (v + r x_m) - \frac{1}{8} p^2 s_m (s_m + 2 r_m) (2 r_m^2 + 2 r_m s_m + s_m^2)$$

Similarly, for the lateral force function $F_{lat}(z)$:

$$v_m \sqrt{u_m^2 + v_m^2} = v_m u + v_m q z + \mathcal{O}\left(\frac{v_m^3}{u}\right)$$

$$f_{lat}(z) = \left((v + r x_m) \left(1 + \frac{r_m^2}{z^2} \right) - p z \right) u + \left((v + r x_m) \left(1 + \frac{r_m^2}{z^2} \right) - p z \right) q z$$

$$I_{lat} = \int_{z_s}^{z_b} f_{lat}(z) dz$$

$$= \frac{1}{2} (s_m + 2 r_m) u p s_m - \frac{1}{3} (s_m^2 + 3 r_m s_m + 3 r_m^2) q p s_m + \frac{u s_m (s_m + 2 r_m) (v + r x_m)}{r_m + s_m}$$

$$- \frac{1}{2} (v + r x_m) \left(s_m^2 + 2 r_m s_m + 2 r_m^2 \ln \left(\frac{r_m + s_m}{r_m} \right) \right) q$$

$$I_{z_{lat}} = \int_{z_s}^{z_b} z f_{lat}(z) dz$$

$$= -\frac{1}{3} u p s_m (s_m^2 + 3 r_m s_m + 3 r_m^2) + \frac{1}{4} p q s_m (s_m + 2 r_m) (2 r_m^2 + 2 r_m s_m + s_m^2)$$

$$- \frac{1}{2} u (v + r x_m) \left(s_m^2 + 2 r_m s_m + 2 r_m^2 \ln \left(\frac{r_m + s_m}{r_m} \right) \right)$$

$$+ \frac{1}{3} s_m q (s_m^2 + 3 r_m s_m + 6 r_m^2) (v + r x_m)$$

Note that force derivatives are easily obtained from these integrated functions because the terms are all linear in products of two velocities. If derivatives for the mast surface and base forces are also required, then those forces should be calculated using the f_{ax}

and f_{lat} functions instead of the F_{ax} and F_{lat} functions. For example, the mast drag contribution X_d to dimensionless axial force X is:

$$\begin{aligned}
X_d &= - \left(\frac{d_s u_m \sqrt{u_m^2 + v_m^2}}{U^2} \right)_{z=z_s} - \left(\frac{d_b u_m \sqrt{u_m^2 + v_m^2}}{U^2} \right)_{z=z_b} - \int_{z_s}^{z_b} \frac{d_{pm} u_m \sqrt{u_m^2 + v_m^2}}{U^2} dz \\
&= - \frac{d_s f_{ax}(z_s)}{U^2} - \frac{d_b f_{ax}(z_b)}{U^2} - \frac{d_{pm} I_{ax}}{U^2} \\
&= \frac{X_d}{U^2} \frac{u^2}{uu} + \frac{X_d}{U^2} \frac{u q l}{uq} + \frac{X_d}{U^2} \frac{q^2 l^2}{qq} + \dots
\end{aligned}$$

which allows the dimensionless derivatives X_d , X_d , etc. used by Feldman [6] to be obtained.

A second order representation is usually adequate for describing the hydrodynamics of a vehicle for simulation purposes (excluding extreme maneuvers). This is thought to be particularly true for Dorado since its main purpose is to ensure the *stability* of the sonar it is towing. We check the accuracy of the f_{ax} and f_{lat} truncated expansions by comparing them with their accurate F_{ax} and F_{lat} parents in a worst case situation. For the mast, the expansions are least accurate where the qz and v_m velocities are largest. This is at the surface where $z = z_s$. During a typical DOLPHIN 10 knot maneuver ($u = 5$ m/s), full scale trials results show that p, q, r maximum magnitudes may be as large as 0.3, 0.17, 0.5 rad/s in some situations. Combining these magnitudes in the worst possible way in the F_{ax} , F_{lat} , f_{ax} , f_{lat} functions and assuming $z_s = -3.5$ m, we find:

$$\frac{f_{ax}(-3.5)}{F_{ax}(-3.5)} = 1.001$$

$$\frac{f_{lat}(-3.5)}{F_{lat}(-3.5)} = .9610$$

so that the truncated terms in the f_{ax} and f_{lat} functions are not significant for Dorado.

Dimensionless Mast Drag Forces

The dimensionless mast drag forces are:

$$\begin{aligned}
 X_d &= -\frac{d_s F_{ax}(z_s)}{U^2} - \frac{d_b F_{ax}(z_b)}{U^2} - \frac{d_{pm} I_{ax}}{U^2} \\
 Y_d &= -\frac{d_s F_{lat}(z_s)}{U^2} - \frac{d_b F_{lat}(z_b)}{U^2} - \frac{d_{pm} I_{lat}}{U^2} \\
 Z_d &= 0 \\
 K_d &= \frac{d_s z_s F_{lat}(z_s)}{U^2 l} + \frac{d_b z_b F_{lat}(z_b)}{U^2 l} + \frac{d_{pm} I z_{lat}}{U^2 l} \\
 M_d &= -\frac{d_s z_s F_{ax}(z_s)}{U^2 l} - \frac{d_b z_b F_{ax}(z_b)}{U^2 l} - \frac{d_{pm} I z_{ax}}{U^2 l} \\
 N_d &= -\frac{d_s x_m F_{lat}(z_s)}{U^2 l} - \frac{d_b x_m F_{lat}(z_b)}{U^2 l} - \frac{d_{pm} x_m I_{lat}}{U^2 l}
 \end{aligned}$$

The X_d and M_d expressions here give the Dorado mast drag at 10 knots as 481 lb (with $z_0 = 3$ m), up from 353 lb for the DOLPHIN Mk1 vehicle ($z_0 = 2.9$ m) at the same speed. The center of action of this drag is 2.7 m above the hull centerline, or a third of a meter below the surface. This reflects the fact that ventilation, spray, and wave drag account for about 3/4 of the mast drag and they are assumed to act right at the surface.

An examination of the other formulae shows that the pitching and rolling moments vary at least lineary with the mast wetted length s_m , and at least quadratically for angular velocity motions.

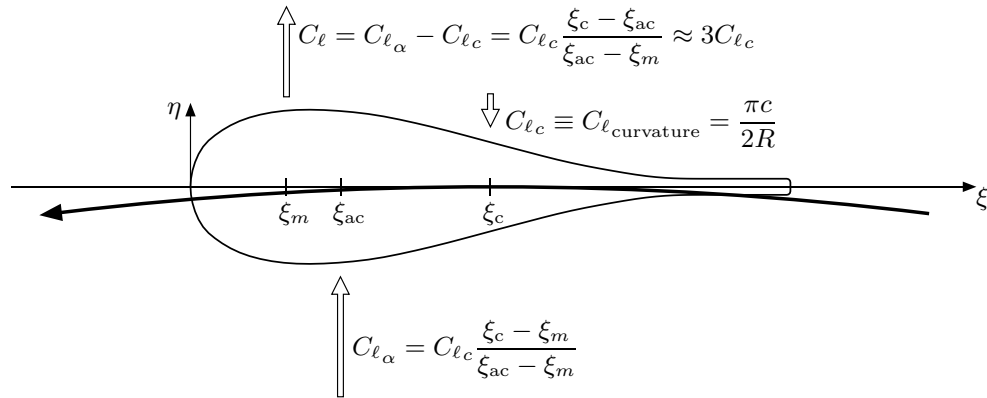
Mast Lift

In translational flow, it is assumed that the self-aligning fairings self-align, generating no lift forces (forces perpendicular to the local flow). In rotational flow, the fairings still self-align (ie, no moment is sustained at the pivot point, neglecting friction), but lift is still generated because of the effective ‘camber’ of the symmetrical fairing in the curved streamlines. This effect has been analyzed by Watt [13] who uses thin airfoil theory to show:

- The lift from the curved streamlines acts at the midchord point x_c and is directed towards the center of curvature.
- The 2D curvature lift coefficient (based on chord length) is $C_l = \pi c/2R$, where c is the fairing chord length and R is the streamline radius of curvature.

- These thin airfoil theory predictions agree with Reynolds Averaged Navier-Stokes (RANS) predictions to within 8%.
- The curvature lift deflects the fairing midchord towards the center of curvature, creating an angle of attack α which generates a lift at the quarter chord (the ‘aerodynamic center’ x_{ac}) directed away from the center of curvature (see figure 5). Equilibrium is achieved when the moment about the mast pivot point x_m (which coincides with ξ_m) is zero.

Fig. 5: Streamline Curvature Induced Side Force on the Dorado Self-Aligning Fairing



Thus, the net force on the self-aligning fairing is several times larger than the original curvature lift and in the opposite direction. Note that the amplification shown here is very sensitive to the correct determination of the aerodynamic center since the lift is inversely proportional to $(\xi_{ac} - \xi_m)$ which is a small quantity.

A possible problem with self-aligning fairings is that they are subject to friction at the pivot point. These fairings actually pivot about the hollow snorkel which has a radius about equal to $\xi_m - \xi_{ac}$. So the friction acts with the same moment arm as the incidence lift C_{l_α} . In the past, it has been assumed that friction would act to oppose deflection by C_{l_c} thereby reducing the magnitude of C_{l_α} . Comparisons with trials results [10] and thin airfoil theory predictions of C_{l_c} , ξ_c , and ξ_{ac} suggested that an

empirical correction factor of 0.8 accounted for this effect. However, the RANS predictions of these quantities [13] suggest $\xi_c = 0.46$ instead of 0.5 and $\xi_{ac} = 0.254$ instead of 0.25 (thin airfoil theory and RANS predictions of C_{lc} agree well).

Although these are only small differences, when used in the expression for C_l below, they eliminate the need for the empirical correction factor. Thus, the RANS predictions for these quantities are used below. One assumes, then, that friction is not important.

Therefore, the net side force, quoted as a 2D lift coefficient nondimensionalized by chord length, is:

$$C_l = \frac{1}{2} \frac{\pi c (\xi_c - \xi_{ac})}{R (\xi_{ac} - \xi_m)}$$

This is converted to standard dimensionless form (per meter of submerged mast length) in:

$$f_c = \frac{C_l c}{l^2}$$

$$= \frac{f_0}{R}$$

where f_0 is dimensionless:

$$f_0 = \frac{C_l c R}{l^2}$$

$$= \frac{1}{2} \frac{\pi c^2 (\xi_c - \xi_{ac})}{(\xi_{ac} - \xi_m) l^2}$$

RANS calculations [13] give the following ξ_c and ξ_{ac} values, allowing f_0 to be evaluated:

$$\xi_c = .46 c, \quad \xi_{ac} = .254 c, \quad \xi_m = .1776 c, \quad c = .6223, \quad l = 8.2$$

$$f_0 = .02439$$

The radius of streamline curvature at the mast is the velocity component in the horizontal plane divided by the angular rotation in the same plane:

$$R = \frac{\sqrt{u_m^2 + v_m^2}}{r}$$

where R , and therefore f_c , have the sign of the angular velocity r .

As with mast drag, we convert f_c into a local lift by multiplying by $(u_m^2 + v_m^2) / U^2$, the local dynamic pressure contributing to the lift nondimensionalized by the global dynamic pressure. This is then multiplied by the cosine and sine of the local horizontal plane flow angle to give the lateral and axial force components:

$$\begin{aligned} \text{local lateral lift force component} &= -\frac{f_c u_m \sqrt{u_m^2 + v_m^2}}{U^2} \\ &= -\frac{f_0 r u_m}{U^2} \end{aligned}$$

$$\begin{aligned} \text{local axial lift force component} &= \frac{f_c v_m \sqrt{u_m^2 + v_m^2}}{U^2} \\ &= \frac{f_0 r v_m}{U^2} \end{aligned}$$

This analysis ignores the second order induced drag from f_c , which is proportional to the square of the lift divided by the aspect ratio: $O((f_0 r)^2 / a)$, where a is the aspect ratio. Although the Dorado mast has a submerged aspect ratio only of about 5, it has the hull on one end and the free surface on the other and so effectively has a larger aspect ratio. This, together with the fact that $f_0 \ll 1$, suggests that neglecting the induced drag term is justified.

The dimensionless lift forces can now be calculated.

$$X_l = \int_{z_s}^{z_b} \frac{f_0 r \left((v + r x_m) \left(1 + \frac{r_m^2}{z^2} \right) - p z \right)}{U^2} dz$$

$$= \frac{1}{2} \frac{f_0 s_m (s_m + 2 r_m) (2 v r + (r_m + s_m) p r + 2 r^2 x_m)}{U^2 (r_m + s_m)}$$

$$= \frac{X_l \text{ } vr l}{U^2} + \frac{X_l \text{ } pr l^2}{U^2} + \frac{X_l \text{ } r^2 l^2}{U^2}$$

where this last form can be used to identify coefficients, if required. Since many of these coefficients are not now required in a simulation, so that new programming would be required to accomodate them, it is easier just to evaluate the entire dimensionless X_l force, the second line above, in a subroutine that calculates all the mast effects (Appendix C).

Similarly:

$$Y_l = \int_{z_s}^{z_b} - \frac{f_0 r (u + q z)}{U^2} dz$$

$$= \frac{1}{2} \frac{s_m f_0 (-2 u r + q r (s_m + 2 r_m))}{U^2}$$

$$Z_l = 0$$

$$K_l = \int_{z_s}^{z_b} \frac{z f_0 r (u + q z)}{U^2 l} dz$$

$$= - \frac{1}{2} \frac{(s_m + 2 r_m) s_m f_0 u r}{U^2 l} + \frac{\frac{1}{3} s_m f_0 (s_m^2 + 3 r_m s_m + 3 r_m^2) q r}{U^2 l}$$

$$M_l = \int_{z_s}^{z_b} \frac{z f_0 r \left((v + r x_m) \left(1 + \frac{r_m^2}{z^2} \right) - p z \right)}{U^2 l} dz$$

$$= -\frac{1}{2} \frac{f_0 \left(s_m^2 + 2 r_m s_m + 2 r_m^2 \ln \left(\frac{r_m + s_m}{r_m} \right) \right) r (v + r x_m)}{U^2 l}$$

$$- \frac{1}{3} \frac{f_0 s_m (s_m^2 + 3 r_m s_m + 3 r_m^2) p r}{U^2 l}$$

$$N_l = \frac{Y_l x_m}{l}$$

$$N_l = \frac{1}{2} \frac{s_m x_m f_0 (-2 u r + q r (s_m + 2 r_m))}{U^2 l}$$

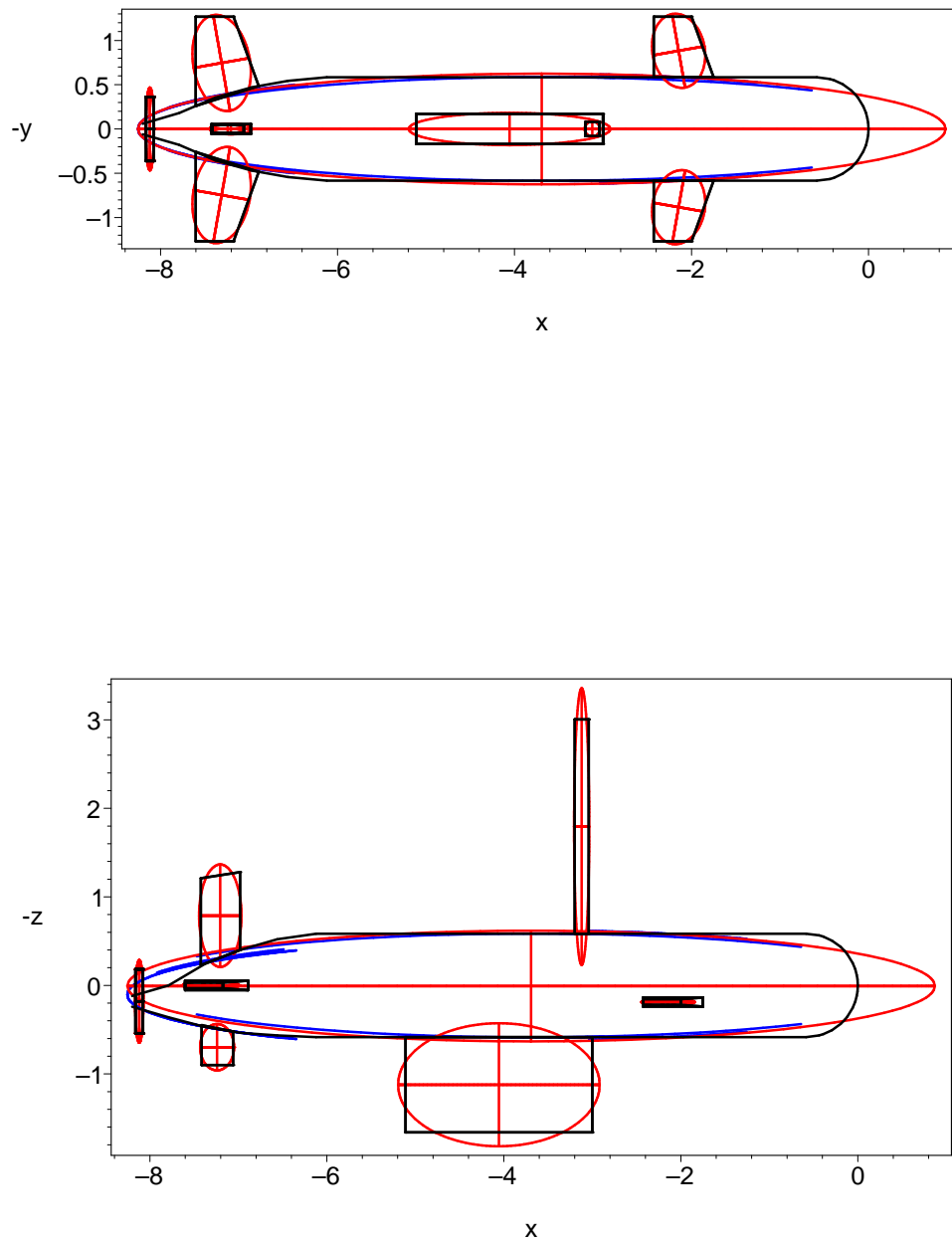
The rotation lift generated by the mast increases the K_r derivative for the mastless vehicle (Appendix B) by 270%. It explains large roll excursions that occurred in earlier versions of the vehicle which lacked the static stability of the current Dorado vehicle.

And note that the K_r derivative varies with s_m^2 , indicating the necessity for modelling the effect of depth.

Unsteady (Added Mass) Derivatives

The ESAM program [5] predicts the added mass coefficients based solely on input geometry. Its input file is shown in Appendix A. The specified input geometry is shown in black in figure 6 below. ESAM calculates added mass by replacing each vehicle component with an equivalent ellipsoid, shown in red in the figure. The effect of the velocity field from the hull on appendages is accounted for by using hull replacement ellipsoids with geometry optimized to each appendage; portions of these locally optimized ellipsoids are shown in blue.

Fig. 6: Dorado ESAM Input (black) and Ellipsoid (red) Geometry



ESAM processes the vehicle component by component. Unlike DERIVS, however, the mast can be included in the ESAM calculation. Although the mast is covered with

self-aligning fairings, its added mass contribution can be estimated by assuming the fairings always align with the local flow. And since the added mass of a cylinder is primarily determined by its dimension normal to the local flow, it suffices to add a cylinder to the top of the hull with a diameter equal to the maximum thickness of the fairings and a length equal to the average depth of the water over the hull (we assume $z_0 = 3$ m - see figure 4).

The propeller guard (essentially a ring wing) makes a very small contribution to the added mass. It is modelled here as a box with ellipsoids making up each side. The length of each side is 1/4 the circumference of the propeller guard.

The overall added mass coefficients predicted by ESAM are:

\dot{u}	\dot{v}	\dot{w}	\dot{p}	\dot{q}	\dot{r}	
-1.391E-03	0.000E+00	2.187E-05	0.000E+00	1.957E-05	0.000E+00	X
	-3.587E-02	0.000E+00	9.979E-04	0.000E+00	7.051E-04	Y
		-2.905E-02	0.000E+00	-5.780E-04	0.000E+00	Z
			-1.558E-04	0.000E+00	-2.667E-05	K
				-1.822E-03	0.000E+00	M
					-1.578E-03	N

This matrix gives the unsteady derivatives by matching a force on the right (one of the 6 rows) with an acceleration on top (one of the 6 columns). The matrix is symmetric so it is redundant to show derivatives below the diagonal. The component contributions that make up these totals are shown on the next page.

There remains the issue of the effect of variable depth on added mass. That is, what is the effect of variable wetted mast length on these coefficients, an effect that is accounted for in the steady state coefficients? This is ascertained by increasing the length of the mast (effectively the wetted mass length s_m) by 10% in the ESAM input file and rerunning the code. The coefficient changes that result are all less than 2% except for the $X_{qdot} = M_{udot}$ derivatives which change by 35%. However, in the equations of motion, the X_{qdot}, M_{udot} coefficients are always paired with a $m z_G$ term, where m is vehicle mass and z_G is the vehicle center of mass location along the z axis. Since Dorado's $m z_G$ term is more than 100 times larger than the change in X_{qdot}, M_{udot} obtained by lengthening the mast 10%, we can neglect this change.

Thus, the equations of motion are insensitive to changes in the added mass coefficients that result from varying wetted mast length. As a result, the added mass coefficients do not need to account for varying depth. The coefficients do, of course, account for the nominal mast length, assuming $z_0 = 3$ m.

ESAM (version 1.42) output file on 02-Oct-02 at 15:50:44 hrs.
 The input file is: ~/MCM/RMV/Dorado/Derivs/Build3/esam.inp
 A 13 component body.

THE DIMENSIONLESS ADDED MASSES; the reference length = 8.200000

component	type	Xud	Xvd,Yud	Xwd,Zud	Xpd,Kud	Xqd,Mud	Xrd,Nud	Nrd
Hull	hp	-0.0009087353	0.0000000000	0.0000000000	0.0000000000	-0.0000008232	0.0000000000	-0.0013951687
StbdForepln	1s	-0.0000105089	-0.0000001869	0.0000037531	0.0000002964	-0.0000008402	0.0000007129	-0.0000004653
PortForepln	1s	-0.0000105089	0.0000001869	0.0000037531	-0.0000002964	-0.0000008402	-0.0000007129	-0.0000004653
StbdSternpln	1s	-0.0000162419	-0.0000034912	0.0000087788	0.0000006386	0.0000036844	0.0000026462	-0.0000017076
PortSternpln	1s	-0.0000162419	0.0000034912	0.0000087788	-0.0000006386	0.0000036844	-0.0000026462	-0.0000017076
Rudder	1s	-0.0000070666	0.0000000000	-0.0000016487	0.0000000000	-0.0000010920	0.0000000000	-0.0000338170
VertStabilizr	1s	-0.0000275018	0.0000000000	0.0000037440	0.0000000000	0.0000036360	0.0000000000	-0.0001017704
Keel	1s	-0.0002181763	0.0000000000	-0.0000038160	0.0000000000	-0.0000236842	0.0000000000	-0.0000336882
PropGuards	3n	-0.0000000092	0.0000000000	0.0000000000	0.0000000000	-0.0000000002	0.0000000004	-0.0000042532
PropGuardp	3n	-0.0000000092	0.0000000000	0.0000000000	0.0000000000	-0.0000000002	-0.0000000004	-0.0000042532
PropGuardt	3n	-0.0000000092	0.0000000000	0.0000000000	0.0000000000	0.0000000002	0.0000000000	-0.0000000001
PropGuardb	3n	-0.0000000092	0.0000000000	0.0000000000	0.0000000000	-0.0000000006	0.0000000000	-0.0000000001
Mast	1s	-0.0001758907	0.0000000000	-0.0000014721	0.0000000000	0.0000358501	0.0000000000	-0.0000009597
=====								
TOTALS		-0.0013909092	0.0000000000	0.0000218711	0.0000000000	0.0000195741	0.0000000000	-0.0015782564
=====								
component	type	Yvd	Ywd,Zvd	Ypd,Kvd	Yqd,Mvd	Yrd,Nvd	Mqd	Mrd,Nqd
Hull	hp	-0.0253417740	0.0000000000	0.0000229571	0.0000000000	-0.0000256869	-0.0013951694	0.0000000000
StbdForepln	1s	-0.0000129153	0.0000886604	0.0000071426	-0.0000161013	-0.0000023042	-0.0000240652	-0.0000028089
PortForepln	1s	-0.0000129153	-0.0000886604	0.0000071426	0.0000161013	-0.0000023042	-0.0000240652	0.0000028089
StbdSternpln	1s	-0.0000078196	-0.0000516772	-0.0000038172	-0.0000219443	0.0000035660	-0.0001781714	0.0000088000
PortSternpln	1s	-0.0000078196	0.0000516772	-0.0000038172	0.0000219443	0.0000035660	-0.0001781714	-0.0000088000
Rudder	1s	-0.0001973918	0.0000000000	0.0000119829	0.0000000000	0.0000816946	-0.0000004150	0.0000000000
VertStabilizr	1s	-0.0005982148	0.0000000000	-0.0000480363	0.0000000000	0.0002466968	-0.0000012560	0.0000000000
Keel	1s	-0.0094579572	0.0000000000	0.0010444720	0.0000000000	0.0003980295	-0.0000035727	0.0000000000
PropGuards	3n	-0.0000146385	0.0000000000	0.0000003213	0.0000000000	0.0000078905	-0.0000000001	0.0000000000
PropGuardp	3n	-0.0000146385	0.0000000000	0.0000003213	0.0000000000	0.0000078905	-0.0000000001	0.0000000000
PropGuardt	3n	-0.0000000002	0.0000000000	0.0000000000	0.0000000000	0.0000000001	-0.0000042532	0.0000000000
PropGuardb	3n	-0.0000000002	0.0000000000	0.0000000000	0.0000000000	0.0000000001	-0.0000042533	0.0000000000
Mast	1s	-0.0002018634	0.0000000000	-0.0000407212	0.0000000000	-0.0000139188	-0.0000085225	0.0000000000
=====								
TOTALS		-0.0358679483	0.0000000000	0.0009979480	0.0000000000	0.0007051201	-0.0018219155	0.0000000000
=====								
component	type	Zwd	Zpd,Kwd	Zqd,Mwd	Zrd,Nwd	Kpd	Kqd,Mpd	Krd,Npd
Hull	hp	-0.0253417740	0.0000000000	0.0000256869	0.0000000000	-0.0000000208	0.0000000000	0.0000000233
StbdForepln	1s	-0.0007270707	-0.0000582868	0.0001320909	0.0000155290	-0.0000048221	0.0000105739	0.0000012517
PortForepln	1s	-0.0007270707	0.0000582868	0.0001320909	-0.0000155290	-0.0000048221	-0.0000105739	0.0000012517
StbdSternpln	1s	-0.0009874937	-0.0000733788	-0.0004193077	0.0000207162	-0.0000058846	-0.0000312138	0.0000015305
PortSternpln	1s	-0.0009874937	0.0000733788	-0.0004193077	-0.0000207162	-0.0000058846	0.0000312138	0.0000015305
Rudder	1s	-0.0000017884	0.0000000000	-0.0000008424	0.0000000000	-0.0000007412	0.0000000000	-0.0000049594
VertStabilizr	1s	-0.0000048025	0.0000000000	-0.0000023001	0.0000000000	-0.0000041904	0.0000000000	0.0000198096
Keel	1s	-0.0002423604	0.0000000000	-0.0000106616	0.0000000000	-0.0001200035	0.0000000000	-0.0000439556
PropGuards	3n	-0.0000000002	0.0000000000	-0.0000000001	0.0000000000	-0.0000000163	0.0000000000	-0.0000001732
PropGuardp	3n	-0.0000000002	0.0000000000	-0.0000000001	0.0000000000	-0.0000000163	0.0000000000	-0.0000001732
PropGuardt	3n	-0.0000146385	0.0000000000	-0.0000078905	0.0000000000	-0.0000000092	0.0000000000	0.0000000000
PropGuardb	3n	-0.0000146385	0.0000000000	-0.0000078905	0.0000000000	-0.0000000092	0.0000000000	0.0000000000
Mast	1s	-0.0000011091	0.0000000000	0.0000003770	0.0000000000	-0.0000094247	0.0000000000	-0.0000028078
=====								
TOTALS		-0.0290502406	0.0000000000	-0.0005779551	0.0000000000	-0.0001558449	0.0000000000	-0.0000266719

Concluding Remarks

The hydrodynamic forces on the Dorado Build 3 vehicle are estimated and provided in a form that can be used in a six degree-of-freedom vehicle simulation. The forces apply to either old or new versions of the fore and sternplanes. The drag and lift of the snorkel mast are accounted for as functions of vehicle depth.

The force estimates for all but the mast effects are provided as hydrodynamic coefficients (first and second order derivatives). The steady state coefficients are estimated using the DERIVS/DSSP20 programs, but corrections must be made to the depth, pitch, yaw, and roll control derivatives. The ESAM program is used to estimate unsteady (added mass) effects. The lift and drag of the mast self-aligning fairings are estimated using a rational model. Of particular interest is the lift developed by the self-aligning fairings in turns because of curvature in the onset streamlines; this lift is reversed and amplified by the self-alignment mechanism.

In calculating the roll control derivatives, it became evident that implementing roll control via sternplanes is inefficient. An aileron type control surface on the mast would have more leverage with much less interference, and should therefore provide better roll control.

References

- [1] D.A. Hopkin, G.D. Watt, and M.L. Seto, *The Development of a Semi-Submersible Vehicle for Use in Minehunting Applications*, RTO AVT Symposium on Unmanned Vehicles for Aerial, Ground, and Naval Military Operations, Turkey, October 2000.
- [2] G.D. Watt, *Dorado Build 1 Fore and Sternplane Redesign*, DREA TM 2002-048, June 2002.
- [3] G.D. Watt, *Estimating Underwater Vehicle Stability and Control Derivatives Using ESAM and a Preliminary Version of DSSP20*, DREA TM 98/224, September 1998.
- [4] M. Mackay, *DSSP20 (Beta Edition) User Guide to the Preprocessing Modules*, DREA TM 1999-108, August 1999.
- [5] G.D. Watt, *Estimates for the Added Mass of a Multi-Component, Deeply Submerged Vehicle*, DREA TM 88/213, October 1988.
- [6] J. Feldman, *DTNSRDC Revised Standard Submarine Equations of Motion*, DTNSRDC/SPD-0393-09, June 1979.
- [7] G.D. Watt, M. Seto, and T. Brockett, *Hydrodynamic Considerations for Semi-Submersible Minehunting Vehicles*, Fourth Canadian Marine Hydrodynamics and Structures Conference, Ottawa, June 1997.
- [8] W.C. Pitts, J.N. Nielsen, G.E. Kaattari, *Lift and Center of Pressure of Wing-Body-Tail Combinations at Subsonic, Transonic, and Supersonic Speeds*, NACA Report 1307, 1957.
- [9] J. De Young, *Spanwise Loading For Wings and Control Surfaces of Low Aspect Ratio*, NACA Technical Note 2011, January 1950.
- [10] G.J. Adams and D.W. Dugan, *Theoretical Damping in Roll and Rolling Moment Due to Differential Wing Incidence for Slender Cruciform Wings and Wing-Body Combinations*, NACA Report 1088, 1952.
- [11] L.F. Whicker and L.F. Fehlner, *Free-Stream Characteristics of a Family of Low-Aspect-Ratio, All-Movable Control Surfaces for Application to Ship Design*, DTMB Report 933, December 1958.
- [12] S.F. Hoerner and H.V. Borst, **Fluid-Dynamic Lift**, published by the authors, 1975.
- [13] G.D. Watt, *A Fairing Rotating About a Distant Axis*, CFD2001, the 9th Annual Conference of the CFD Society of Canada, Waterloo, May 2001.

Appendix A: The Dorado DSSP20 and ESAM Input Files

The DSSP20 and ESAM input files listed below are used by these programs for estimating the steady and unsteady 6 DOF hydrodynamic characteristics of a vehicle. This is done by evaluating the vehicle components one at a time and, where possible, accounting for interference between components.

DSSP20

The DSSP20 input file is described in detail by Mackay [4]. This input does not account for the presence of the mast.

Title DORADO vehicle, Build 3 configuration.

Plot
Maple

Reference
-3.7 0.0 0.0 ! reference is on hull axis opposite nominal CB
0.0 0.0 0.0

Hull
Label #Hull
Station ! z camber relative to x-axis
0.000 0.000 0.0000 0.0 ! 0.0
1.115 1.115 0.9764 -.009 ! 0.0
1.1684 1.1684 1.0722 -.018 ! 0.0
1.1684 1.1684 1.0722 -.027 ! 0.0
1.1684 1.1684 1.0722 -.036 ! 0.0
1.1684 1.1684 1.0722 -.045 ! 0.0
1.1684 1.1684 1.0722 -.054 ! 0.0
1.1684 1.1684 1.0722 -.063 ! 0.0
1.1684 1.1684 1.0722 -.072 ! 0.0
1.1684 1.1684 1.0722 -.081 ! 0.0
1.1684 1.1684 1.0722 -.090 ! 0.0
1.1684 1.1684 1.0722 -.099 ! 0.0
1.1684 1.1684 1.0722 -.108 ! 0.0
1.1684 1.1684 1.0722 -.117 ! 0.0
1.1684 1.1684 1.0722 -.126 ! 0.0
1.1684 1.1684 1.0722 -.135 ! 0.0
1.086 1.086 0.9263 -.122 ! 0.022
0.94 0.94 0.6940 -.086 ! 0.067
0.71 0.71 0.3959 -.049 ! 0.113
0.36 0.36 0.1018 .009 ! 0.18
0.12 0.12 0.0113 0.0 ! 0.18
Nose 0.0
Tail -8.2 0.0 0.18

Lift
Label #StarboardSternplane
Sternplane 0.39 0.5842
TailEff 0.7772 ! Dempsey
AllMoving 0.84
Planform
-6.8901 .4842 0.0
-7.1756 1.2685 0.0
-7.6021 1.2685 0.0
-7.6021 .2602 0.0
ToC 0.15
Save

Lift
Label #PortSternplane

Reflected

Lift
Label #StarboardForeplane
SBowplane 0.5842
AllMoving 1.0
Planform
-1.7508 0.5842 0.188
-1.9999 1.2685 0.188
-2.4264 1.2685 0.188
-2.4264 0.5842 0.188
ToC 0.15
Save

Lift
Label #PortForeplane
Reflected

Lift
Label #Rudder
Rudder 0.395 0.5842
TailEff 0.6964 ! Dempsey
AllMoving 0.92
Planform
-7.06 0.00 0.52
-7.06 0.00 0.9
-7.416 0.00 0.9
-7.416 0.00 0.45
ToC 0.25
HasEndP 0.125 1

Lift
Label #VerticalStabilizer
Tail 0.4 0.5842
TailEff 0.768 ! Dempsey
Planform
-6.98 0.00 -0.4
-6.98 0.00 -1.28
-7.425 0.00 -1.21
-7.425 0.00 -0.23
ToC 0.25

Lift
Label #Keel
Sail 0.5842
Planform
-3.0 0.0 0.5842
-3.0 0.0 1.66
-5.112 0.0 1.66
-5.112 0.0 0.5842
ToC 0.16

ESAM

The ESAM input file is described in detail by Watt [5]. This input does account for the mast, assuming a nominal vehicle depth of 3 m.

```
13 Dorado, Build 3
P
-3.7      put reference at nominal CB
0.0
8.2
132
hp  Hull
/
18
-8.2      0.12      0.12      0.18
-7.79     0.36      0.36      0.18
-7.38     0.71      0.71      0.113
-6.97     0.94      0.94      0.067
-6.56     1.086     1.086     0.022
-6.1214   1.1684    1.1684    0.0
-0.5842   1.1684    1.1684    0.0
-0.4382   1.1313    1.1313    0.0
-0.3895   1.1016    1.1016    0.0
-0.2921   1.0119    1.0119    0.0
-0.1947   0.8708    0.8708    0.0
-0.1461   0.7729    0.7729    0.0
-0.1168   0.7009    0.7009    0.0
-0.0584   0.5092    0.5092    0.0
-0.0292   0.3648    0.3648    0.0
-0.012    0.2356    0.2356    0.0
-0.004    0.1365    0.1365    0.0
0.0       0.0       0.0       0.0
1s  StbdForepln
-2.4264 0.5842 0.188 0.0 0.6756 0.0 0.4265 0.6843 0.0 0.6843 0.15
1s  PortForepln
-2.4264 -0.5842 0.188 180.0 0.6756 0.0 0.4265 0.6843 0.0 0.6843 0.15
1s  StbdSternpln
-7.6021 0.2602 0.0 0.0 0.712 0.224 0.4265 1.0083 0.0 1.0083 0.15
1s  PortSternpln
-7.6021 -0.2602 0.0 180.0 0.712 0.224 0.4265 1.0083 0.0 1.0083 0.15
1s  Rudder
-7.416 0.0 0.45 90.0 0.356 0.07 0.356 0.45 0.0 0.45 0.25
1s  VertStabilizr
-7.425 0.0 -0.23 -90.0 0.445 0.17 0.445 1.05 0.0 0.98 0.25
1s  Keel
-5.112 0.0 0.5842 90.0 2.112 0.0 2.112 1.0758 0.0 1.0758 0.16
3n  PropGuards
-8.1625 .3613 0.18 -90.0 .085 0,.3613 .085 0,-.3613 .085 .025
3n  PropGuardp
-8.1625 -.3613 0.18 90.0 .085 0,.3613 .085 0,-.3613 .085 .025
3n  PropGuardt
-8.1625 0.0 -0.1813 0.0 .085 0,.3613 .085 0,-.3613 .085 .025
3n  PropGuardb
-8.1625 0.0 0.5413 180.0 .085 0,.3613 .085 0,-.3613 .085 .025
1s  Mast
-3.2 0.0 -0.5842 -90.0 0.159 0.0 0.159 2.42 0.0 2.42 1.0
```

Appendix B: The Dorado Mastless Steady State Derivatives

This is the output from DERIVS incorporating the corrections to drag (x^*), the small Z_w , M_w , Z_q , and M_q corrections resulting from the foreplane ΔZ_w discrepancy, and the sternplane, rudder, and foreplane control derivative corrections.

CORRECTED Dorado MASTLESS Dimensionless Stability Derivatives: Build 3

X^*, X_{vv}	-0.0036001	0.0690062		$X^*_{old} = -0.0020417$
$X_w, X_{ww}, X_w w $	0.0000184	0.0810214	-0.0014221	
X_{pp}, X_{rr}	-0.0000903	0.0048077		
$X_q, X_{qq}, X_q q $	-0.0001336	0.0093780	0.0001509	
$Y_v, Y_v v $	-0.1530390	-0.1192487		
$Y_p, Y_p p $	0.0108496	0.0000163		
$Y_r, Y_r r $	0.0265862	0.0039736		
Z^*, Z_{vv}	-0.0002779	-0.0001393		
$Z_w, Z_{ww}, Z_w w $	-0.1480168	-0.0135169	-0.1068810	$Z_w_{old} = -0.1592186$
Z_{pp}, Z_{rr}	0.0000000	-0.0000012		
$Z_q, Z_{qq}, Z_q q $	-0.0211099	-0.0012814	-0.0022532	$Z_q_{old} = -0.0187876$
$K_v, K_v v $	0.0079937	0.0042778		
$K_p, K_p p $	-0.0023596	-0.0000016		
$K_r, K_r r $	-0.0005739	-0.0000564		
M^*, M_{vv}	0.0004385	0.0020014		
$M_w, M_{ww}, M_w w $	0.0081326	-0.0020678	-0.0186506	$M_w_{old} = 0.0104549$
M_{pp}, M_{rr}	-0.0000116	-0.0002063		
$M_q, M_{qq}, M_q q $	-0.0165276	-0.0007012	-0.0010120	$M_q_{old} = -0.0170091$
$N_v, N_v v $	-0.0127989	0.0190693		
$N_p, N_p p $	0.0012276	-0.0000021		
$N_r, N_r r $	-0.0070427	-0.0016514		

CORRECTED Dimensionless Control Derivatives

X_{dsds}, Z_{ds}	-0.0022873	-0.0397794		$C_{su} = 0.6990$
$M_{ds}, M_{dsds}, M_{ds} ds $	-0.0165060	0.0000000	-0.0008099	
X_{dodo}, Y_{do}	-0.0010989	0.0000000		$C_{sd} = 0.4845$
K_{do}, M_{dodo}, N_{do}	0.0017758	0.0000000	0.0000000	
X_{dfdf}, Z_{df}	-0.0316288	-0.0442960		$C_f = 1.2032$
$M_{df}, M_{dfdf}, M_{df} df $	0.0094788	-0.0007252	0.0006586	
X_{drdr}, Y_{dr}	0.0001995	0.0056862		$C_{ru} = 0.6281$
K_{dr}, M_{drdr}, N_{dr}	-0.0002683	0.0000106	-0.0023979	$CrK = 0.5602$

Appendix C: Mast Drag and Lift Code

This appendix provides explicit FORTRAN coding for implementing the mast drag and lift hydrodynamic forces derived in the main body of this report.

```

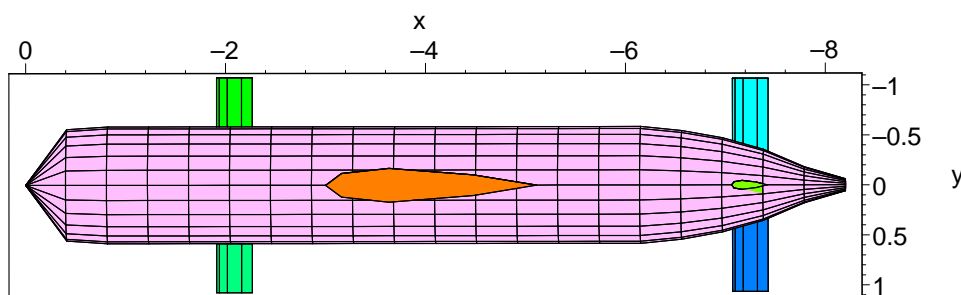
* Assume z0, xm, rm, l (in meters)
*       theta, phi (in radians)
*       u, v, w (in m/s)
*       p, q, r (in radians/s) are all known.
*
* Statement functions
      Fax(z) = (u+q*z)*sqrt((u+q*z)**2+(vrxm*(1+rm**2/z**2)-p*z)**2)
      Flat(z) = (vrxm*(1+rm**2/z**2)-p*z)*sqrt((u+q*z)**2+(vrxm*(1+rm**2
# /z**2)-p*z)**2)
*
      sm = (z0-xm*sin(theta))/cos(theta)/cos(phi)-rm
      zs = -rm-sm
      zb = -rm
      UU2 = u**2+v**2+w**2
      ds = 0.1871249E-2
      db = 0.9249517E-4
      dpmu = 0.1564563E-3/UU2
      f0 = 0.2439302E-1
      vrxm = v+r*xm
      iz2by3 = (sm**2+3*rm*sm+3*rm**2)*sm/3
      iz21by3 = (sm**2+3*rm*sm+6*rm**2)*sm/3
      iz3by4 = rm**2/2+rm*sm/2+sm**2/4
      lnby2 = sm**2/2+rm*sm+rm**2*log((rm+sm)/rm)
      izby2 = (sm+2*rm)*sm/2
      rmsm = rm+sm
      f0rU2 = f0/UU2*r
      dsfaxu = ds*Fax(zs)/UU2
      dbfaxu = db*Fax(zb)/UU2
      dsflatu = ds*Flat(zs)/UU2
      dbflatu = db*Flat(zb)/UU2
      Iax = u**2*sm-2*q*u*izby2+q**2*iz2by3+sm*vrxm**2*(12*rm**3+16*rm*s
# m**2+3*sm**3+24*rm**2*sm)/rmsm**3/6+p*lnby2*vrxm+p**2*iz2by3/2
      Izax = -u**2*izby2+2*q*u*iz2by3-2*q**2*izby2*iz3by4-vrxm**2*(2*lnb
# y2-2*rm*sm-sm**2)/2-2*vrxm**2*izby2*iz3by4/rmsm**2-p*iz21by3*vrxm-
# p**2*izby2*iz3by4
      Ilat = izby2*u*p-iz2by3*q*p+2*u*izby2*vrxm/rmsm-vrxm*lnby2*q
      Izlat = -u*p*iz2by3+2*q*p*izby2*iz3by4-u*vrxm*lnby2+q*iz21by3*vrxm
      Xd = -dsfaxu-dbfaxu-dpmu*Iax
      Yd = -dsflatu-dbflatu-dpmu*Ilat
      Zd = 0
      Kd = (zs*dsflatu+zb*dbflatu+dpmu*Izlat)/l
      Md = -(zs*dsfaxu+zb*dbfaxu+dpmu*Izax)/l
      Nd = xm/l*Yd
      Xl = f0rU2*izby2*(2*v+rmsm*p+2*r*xm)/rmsm
      Yl = f0rU2*(-u*sm+q*izby2)
      Zl = 0
      Kl = f0rU2*(-izby2*u+iz2by3*q)/l
      Ml = -f0rU2*(lnby2*vrxm+iz2by3*p)/l
      Nl = xm/l*Yl

```

Appendix D: Dorado Build 1 Derivatives

This appendix reproduces the corrections to the derivatives assuming Build 1 geometry, as shown below. The only differences between Build 1 and Build 3 geometry are the fore and sternplane shapes. For Build 1, the original Dolphin foreplanes and the lengthened Dolphin Mk 2 sternplanes are used.

Fig. 7: Dorado Build 1 Fore and Sternplane Geometry



Note that both the Build 1 fore and sternplanes use small end plates at their tips (as does the rudder in both the Build 1 and 3 vehicles).

Sternplane Control Derivative Corrections

Sternplane Pitch Control

Let C_{sul} be the correction that needs to be applied to the DERIVS sternplane pitch control (δ_s) derivatives:

$$C_{sul} = \left(\frac{L_{\delta}}{L_{\alpha}} \right)_{correct}$$

$$= \frac{1}{1+\lambda} - \frac{1}{5} \frac{\lambda(1-\lambda)}{(1+\lambda)^2}$$

Then:

$$b = 2.132, \quad d = .884, \quad \lambda = .4146$$

$$C_{su1} = .6826$$

Sternplane Roll Control

The correction C_{sdl} to be applied to DERIVS δ_o derivatives depends only on λ :

$$C_{sdl} = 3 \frac{\text{WBF}(\lambda, A)}{A(1-\lambda^2)^2}$$

$$= .4987$$

Foreplane Control Derivative Corrections

The Dorado foreplanes have small endplates at their tips with height h about 5% of the full span length b . Hoerner and Borst [12] present data showing that end plates increase the effective aspect ratio a by a factor:

$$k_{ep} \left(\frac{h}{b} \right) = 1 + \frac{1.9h}{b} - \frac{.5h^2}{b^2}$$

$$= 1.112$$

for:

$$\frac{h}{b} < 2.5$$

So:

$$\Delta Z_{wl} = -1.8 \frac{(1-\lambda^2)^2 \pi k_{ep} b^2}{\left(1.8 + \cos(\Omega) \sqrt{\frac{k_{ep}^2 a^2}{\cos(\Omega)^4} + 4} \right) l^2}$$

Since:

$$b = 2.1504 \text{ m}$$

$$a = 2.758$$

$$\lambda = .5433$$

$$\Omega = 0.$$

then the foreplane contribution to Z_{wl} is:

$$\Delta Z_{wl} = -.03933$$

Unlike for the the new, larger foreplanes, this agrees almost exactly with the DERIVS/DSSP20 prediction.

Since:

$$\frac{L_{\delta}}{L_{\alpha}} = \frac{1}{1+\lambda} - \frac{1}{5} \frac{\lambda(1-\lambda)}{(1+\lambda)^2}$$

$$= .6271$$

then:

$$Z_{\delta_{fl}} = \left(\frac{1}{1+\lambda} - \frac{1}{5} \frac{\lambda(1-\lambda)}{(1+\lambda)^2} \right) \Delta Z_{wl}$$

$$= -.02467$$

which is 50% larger than the DERIVS/DSSP20 prediction of Z_{δ_f} . That is, the effective DSSP20 prediction for L_{δ}/L_{α} is 0.42 which is again unrealistically low, as was the case for the new foreplanes.

Since we have good Z_w agreement, no corrections are required to the Build 1 values of Z_w , M_w , Z_q , and M_q . The correction to Z_{δ_f} is achieved using the factor:

$$C_{fl} = -.02467 \frac{1}{Z_{\delta_{fl} DSSP20}}$$

$$= 1.490$$

DSSP20 Input File

The Dorado Build 1 DSSP20 input file differs from the Build 3 version in Appendix A only in the definitions of the fore and sternplanes. The Build 1 specifications are shown below.

```
Lift
Label #StarboardSternplane
Sternplane 0.39 0.5842
TailEff 0.722 ! Dempsey
AllMoving 0.9
Planform
-7.07 0.442 0.0
-7.07 1.066 0.0
-7.426 1.066 0.0
-7.426 0.335 0.0
ToC 0.25
HasEndP 0.1 1
Save
```

```
Lift
Label #PortSternplane
Reflected
```

```
Lift
Label #StarboardForeplane
SBowplane 0.5842 0
AllMoving 1.0
Planform
-1.91 0.5842 0.188
-1.91 1.0752 0.188
-2.266 1.0752 0.188
-2.266 0.5842 0.188
ToC 0.25
HasEndP 0.1 1
Save
```

```
Lift
Label #PortForeplane
Reflected
```

Steady State Derivatives

This is the Build 1 output from DERIVS incorporating the corrections to drag (X^*) and the sternplane, rudder, and foreplane control derivatives.

CORRECTED Dorado MASTLESS Dimensionless Stability Derivatives: Build 1

X^*, X_{vv}	-0.0034084	0.0690062		$X^*_{old} = -0.0018500$
$X_w, X_{ww}, X_w w $	0.0000312	0.0509407	-0.0014697	
X_{pp}, X_{rr}	-0.0000412	0.0048082		
$X_q, X_{qq}, X_q q $	-0.0001309	0.0056825	0.0001513	
$Y_v, Y_v v $	-0.1530390	-0.1192487		
$Y_p, Y_p p $	0.0108496	0.0000163		
$Y_r, Y_r r $	0.0265862	0.0039736		
Z^*, Z_{vv}	-0.0002779	-0.0001393		
$Z_w, Z_{ww}, Z_w w $	-0.0820978	-0.0135169	-0.0844093	
Z_{pp}, Z_{rr}	0.0000000	-0.0000012		
$Z_q, Z_{qq}, Z_q q $	-0.0069856	-0.0014308	-0.0017440	
$K_v, K_v v $	0.0079937	0.0042778		
$K_p, K_p p $	-0.0017005	-0.0000013		
$K_r, K_r r $	-0.0005739	-0.0000564		
M^*, M_{vv}	0.0004399	0.0020014		
$M_w, M_{ww}, M_w w $	0.0174362	-0.0023369	-0.0163539	
M_{pp}, M_{rr}	-0.0000114	-0.0002063		
$M_q, M_{qq}, M_q q $	-0.0080125	-0.0006765	-0.0007758	
$N_v, N_v v $	-0.0127989	0.0190693		
$N_p, N_p p $	0.0012276	-0.0000021		
$N_r, N_r r $	-0.0070411	-0.0016514		

CORRECTED Dimensionless Control Derivatives

X_{dsds}, Z_{ds}	0.0023478	-0.0180358		$C_{s1} = 0.6826$
$M_{ds}, M_{dsds}, M_{ds} ds $	-0.0076428	0.0000000	-0.0003596	
X_{dodo}, Y_{do}	0.0012530	0.0000000		$C_{sd1} = 0.4987$
K_{do}, M_{dodo}, N_{do}	0.0007256	0.0000000	0.0000000	
X_{dfdf}, Z_{df}	-0.0192938	-0.0246659		$C_{f1} = 1.4901$
$M_{df}, M_{dfdf}, M_{df} df $	0.0050948	-0.0004423	0.0003834	
X_{drdr}, Y_{dr}	0.0001995	0.0056862		$C_{ru} = 0.6281$
K_{dr}, M_{drdr}, N_{dr}	-0.0002683	0.0000106	-0.0023979	$CrK = 0.5602$

ESAM input file

The Build 1 ESAM input file differs from the Build 3 version of Appendix A only in the definitions of the fore and sternplanes. The Build 1 specifications are shown below.

```

ls StbdForepln
-2.266 0.5842 0.188      0.0  0.356 0.0  0.356 0.491  0.0 0.491  0.25
ls PortForepln
-2.266 -0.5842 0.188    180.0  0.356 0.0  0.356 0.491  0.0 0.491  0.25
ls StbdSternpln
-7.426 0.335 0.0      0.0  0.356 0.107  0.356 0.731  0.0 0.731  0.25
ls PortSternpln
-7.426 -0.335 0.0    180.0  0.356 0.107  0.356 0.731  0.0 0.731  0.25

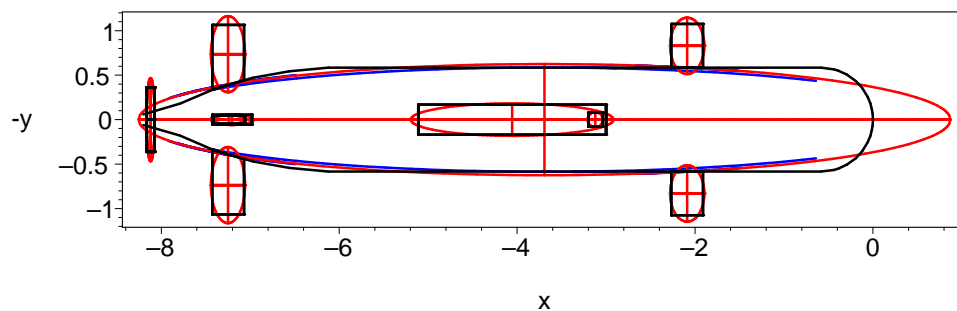
```

Unsteady Derivatives

The ESAM overall added mass coefficients for the Build 1 configuration, followed by the the planform view of the ESAM Build 1 geometry.

\dot{u}	\dot{v}	\dot{w}	\dot{p}	\dot{q}	\dot{r}	
-1.382E-03	0.000E+00	5.510E-06	0.000E+00	1.533E-05	0.000E+00	X
	-3.585E-02	0.000E+00	9.942E-04	0.000E+00	7.031E-04	Y
		-2.673E-02	0.000E+00	-1.621E-04	0.000E+00	Z
			-1.405E-04	0.000E+00	-3.033E-05	K
				-1.541E-03	0.000E+00	M
					-1.576E-03	N

Fig. 8: Build 1 ESAM Input (black) and Ellipsoid (red) Geometry



DOCUMENT CONTROL DATA		
(Security classification of title, body of abstract and indexing annotation must be entered when the overall document is classified)		
1. ORIGINATOR (the name and address of the organization preparing the document.. Organizations for whom the document was prepared, e.g. Establishment sponsoring a contractor's report, or tasking agency, are entered in section 8.)	2. SECURITY CLASSIFICATION (overall security classification of the document including special warning terms if applicable).	
Defence Research and Development Canada – Atlantic PO Box 1012, Dartmouth, N.S. B2Y 3Z7	UNCLASSIFIED	
3. TITLE (the complete document title as indicated on the title page. Its classification should be indicated by the appropriate abbreviation (S,C,R or U) in parentheses after the title).		
Estimating the Hydrodynamic Characteristics of the Dorado Remote Minehunting Vehicle		
4. AUTHORS (Last name, first name, middle initial. If military, show rank, e.g. Doe, Maj. John E.)		
Watt, George D.		
5. DATE OF PUBLICATION (month and year of publication of document)	6a. NO. OF PAGES (total containing information Include Annexes, Appendices, etc).	6b. NO. OF REFS (total cited in document)
October 2002	44	13
7. DESCRIPTIVE NOTES (the category of the document, e.g. technical report, technical note or memorandum. If appropriate, enter the type of report, e.g. interim, progress, summary, annual or final. Give the inclusive dates when a specific reporting period is covered).		
DRDC Atlantic Technical Memorandum		
8. SPONSORING ACTIVITY (the name of the department project office or laboratory sponsoring the research and development. Include address).		
Defence Research and Development Canada – Atlantic, P.O. Box 1012, Dartmouth, Nova Scotia, Canada, B2Y 3Z7		
9a. PROJECT OR GRANT NO. (if appropriate, the applicable research and development project or grant number under which the document was written. Please specify whether project or grant).	9b. CONTRACT NO. (if appropriate, the applicable number under which the document was written).	
11GL-12		
10a ORIGINATOR'S DOCUMENT NUMBER (the official document number by which the document is identified by the originating activity. This number must be unique to this document.)	10b OTHER DOCUMENT NOS. (Any other numbers which may be assigned this document either by the originator or by the sponsor.)	
DRDC Atlantic TM 2002-177		
11. DOCUMENT AVAILABILITY (any limitations on further dissemination of the document, other than those imposed by security classification)		
<input checked="" type="checkbox"/> (x) Unlimited distribution <input type="checkbox"/> () Defence departments and defence contractors; further distribution only as approved <input type="checkbox"/> () Defence departments and Canadian defence contractors; further distribution only as approved <input type="checkbox"/> () Government departments and agencies; further distribution only as approved <input type="checkbox"/> () Defence departments; further distribution only as approved <input type="checkbox"/> () Other (please specify):		
12. DOCUMENT ANNOUNCEMENT (any limitation to the bibliographic announcement of this document. This will normally correspond to the Document Availability (11). However, where further distribution (beyond the audience specified in (11) is possible, a wider announcement audience may be selected).		

13. **ABSTRACT** (a brief and factual summary of the document. It may also appear elsewhere in the body of the document itself. It is highly desirable that the abstract of classified documents be unclassified. Each paragraph of the abstract shall begin with an indication of the security classification of the information in the paragraph (unless the document itself is unclassified) represented as (S), (C), (R), or (U). It is not necessary to include here abstracts in both official languages unless the text is bilingual).

The hydrodynamic forces on the Dorado semi-submersible remote minehunting vehicle are estimated and provided in a form that can be used in a six degree-of-freedom vehicle simulation. The forces apply to either old or new versions of the control planes. The lift (from flow curvature in a turn) and drag of the self-aligning fairings on the snorkel mast are accounted for as a function of vehicle depth. Hydrodynamic coefficients are used for all but the mast effects, where a rational flow model is used. Deficiencies in the control derivatives estimated by the DERIVS/DSSP20 programs are identified and overcome.

14. **KEYWORDS, DESCRIPTORS or IDENTIFIERS** (technically meaningful terms or short phrases that characterize a document and could be helpful in cataloguing the document. They should be selected so that no security classification is required. Identifiers, such as equipment model designation, trade name, military project code name, geographic location may also be included. If possible keywords should be selected from a published thesaurus. e.g. Thesaurus of Engineering and Scientific Terms (TEST) and that thesaurus-identified. If it not possible to select indexing terms which are Unclassified, the classification of each should be indicated as with the title).

hydrodynamic
derivatives
semi-submersible
drone
simulations

Defence R&D Canada

**Canada's leader in defence
and national security R&D**

R & D pour la défense Canada

**Chef de file au Canada en R & D
pour la défense et la sécurité nationale**



www.drdc-rddc.gc.ca